The Cryosphere, 14, 657–672, 2020
https://doi.org/10.5194/tc-14-657-2020

The Cryosphere Open Access EGU

Cryoconite: an efficient accumulator of radioactive fallout in glacial environments

Giovanni Baccolo[1,2], Edyta Łokas[3], Paweł Gaca[4], Dario Massabò[5,6], Roberto Ambrosini[7], Roberto S. Azzoni[7], Caroline Clason[8], Biagio Di Mauro[1], Andrea Franzetti, Massimiliano Nastasi[1,9], Michele Prata[10], Paolo Prati[5,6], Ezio Previtali[1,9], Barbara Delmonte[1], and Valter Maggi[1,2]

[1]Environmental and Earth Sciences Department, University of Milano-Bicocca, Milan, 20126, Italy
[2]INFN section of Milano-Bicocca, Milan, 20126, Italy
[3]Department of Nuclear Physical Chemistry, Institute of Nuclear Physics Polish Academy of Sciences, Cracow, 31-342, Poland
[4]Ocean and Earth Science, University of Southampton, National Oceanography Centre, Southampton, SO14 3ZH, UK
[5]Physics Department, University of Genoa, Genoa, 16146, Italy
[6]INFN section of Genoa, Genoa, 16146, Italy
[7]Department of Environmental Science and Policy, University of Milan, Milan, 20133, Italy
[8]School of Geography, Earth and Environmental Sciences, University of Plymouth, Plymouth, PL48AA, UK
[9]Physics Department, University of Milano-Bicocca, Milan, 20126, Italy
[10]Laboratory of Applied Nuclear Energy, University of Pavia, Pavia, 27100, Italy

Correspondence: Giovanni Baccolo (giovanni.baccolo@unimib.it)

Received: 25 July 2019 – Discussion started: 23 August 2019
Revised: 22 November 2019 – Accepted: 22 January 2020 – Published: 14 February 2020

Abstract. Cryoconite is rich in natural and artificial radioactivity, but a discussion about its ability to accumulate radionuclides is lacking. A characterization of cryoconite from two Alpine glaciers is presented here. Results confirm that cryoconite is significantly more radioactive than the matrices usually adopted for the environmental monitoring of radioactivity, such as lichens and mosses, with activity concentrations exceeding 10 000 Bq kg^{-1} for single radionuclides. This makes cryoconite an ideal matrix to investigate the deposition and occurrence of radioactive species in glacial environments. In addition, cryoconite can be used to track environmental radioactivity sources. We have exploited atomic and activity ratios of artificial radionuclides to identify the sources of the anthropogenic radioactivity accumulated in our samples. The signature of cryoconite from different Alpine glaciers is compatible with the stratospheric global fallout and Chernobyl accident products. Differences are found when considering other geographic contexts. A comparison with data from literature shows that Alpine cryoconite is strongly influenced by the Chernobyl fallout, while cryoconite from other regions is more impacted by events such as nuclear test explosions and satellite reentries. To explain the accumulation of radionuclides in cryoconite, the glacial environment as a whole must be considered, and particularly the interaction between ice, meltwater, cryoconite and atmospheric deposition. We hypothesize that the impurities originally preserved into ice and mobilized with meltwater during summer, including radionuclides, are accumulated in cryoconite because of their affinity for organic matter, which is abundant in cryoconite. In relation to these processes, we have explored the possibility of exploiting radioactivity to date cryoconite.

1 Introduction

Radioecological research is primarily focused on the Earth surface, where continuous atmospheric deposition of fallout radionuclides (FRNs), both natural and artificial, is accumulated. The most common FRNs are cosmogenic nu-

clides, ^{222}Rn progeny and artificial products. The last ones of these have been released into the environment since the second half of the 20th century, as a consequence of nuclear test explosions and accidents. Hundreds of thousands of petabecquerels were spread in the high troposphere and stratosphere from the 1940s to the 1960s, allowing for global dispersion and contamination at the Earth surface. The extent and impact of FRN deposition on the Earth surface is monitored through the analysis of different environmental matrices, which are used to reconstruct FRN deposition (Steinhauser et al., 2013) and understand their environmental mobility and distribution (Avery, 1996; Yasunari et al., 2011). Among the matrices used in the study of FRNs, those that receive the greatest attention share common features: their composition is directly influenced by airborne deposited impurities; the contribution from environmental compartments other than atmosphere is limited; they are widespread, accessible and preferably easy to sample. Given these attributes, lichens, mosses and peat are commonly used to study the distribution of FRNs and establish depositional inventories (Nifontova, 1995; Kirchner and Daillant, 2002).

In recent years cryoconite began drawing attention in the field of radioactive monitoring as an alternative environmental matrix. Cryoconite is the dark, unconsolidated sediment that is found on the surface of glaciers worldwide (Takeuchi et al., 2001). It forms exclusively at the ice–atmosphere interface and in the presence of meltwater. It can be found as a dispersed material on the ice surface or as a deposit accumulated on the bottom of characteristic water-filled holes melted into ice, usually aggregated into granules (cryoconite holes; see Fig. 1). Cryoconite forms out of the interaction between the mineral particles present on the ice surface (both allochthonous and autochthonous) and the complex microbial communities that develop on the surface of glaciers (Cook et al., 2015). Among the microbes that are present on glaciers, cyanobacteria play a major structural role (Langford et al., 2010). During the ablation season, when liquid water is available at the surface of glaciers, cyanobacteria develop films and filaments that promote the formation of aggregates composed of mineral sediments and organic matter, resulting in cryoconite granules (Takeuchi et al., 2001). The composition of cryoconite is dominated by a mineral component accounting for 85 %–95 % of its mass, whereas the remnant fraction is comprised of both living and dead organic matter and is responsible for its dark color (Cook et al., 2015). The formation of cryoconite holes is attributable to the dark color, and thus low albedo, of cryoconite, which enhances the absorption of solar radiation and locally increases ice melting to foster the development of holes in the ice surface. Due to its contribution to ice melting, its diverse composition and the role in biodiversity, cryoconite has been studied by a range of disciplines, including glaciology, microbiology, biogeochemistry and ecology (Takeuchi et al., 2001; Langford et al., 2010; Cook et al., 2015; Ferrario et al., 2017; Pittino et al., 2018a). More recently cryoconite has been the subject of renewed interest due to its ability to accumulate specific substances, including anthropogenic contaminants (Pittino et al., 2018b).

To the best of our knowledge, the first evidence of the accumulation of radionuclides in cryoconite was reported by Tomadin et al. (1996), who found high levels of anthropogenic radioactivity in cryoconite samples from the European Alps. Meese et al. (1997) analyzed cryoconite formed on the surface of multi-year Arctic sea ice, measuring high radioactivity values. Similar observations were successively reported by Cota et al. (2006), who founded unexpectedly high radioactivity burdens (related to ^{137}Cs, ^{210}Pb and ^{7}Be) in cryoconite from the surface of multi-year sea ice in the Canadian Arctic. Since then no other studies (to our knowledge) have focused on the radioactivity of cryoconite until the presentation of an extensive characterization of samples from an Austrian glacier in 2009 (Tieber et al., 2009). That study has showed that cryoconite is contaminated not only by ^{137}Cs, a common artificial radionuclide spread into the environment, but also by several other species, artificial and natural in origin. The reported activity levels in this study are extremely high and comparable to soil samples from nuclear incident and explosion sites (Steinhauser et al., 2014; Abella et al., 2019). Subsequent studies, carried out in different regions of the global cryosphere (Alps, Caucasus, Svalbard and Canada), corroborated the ability of cryoconite to accumulate radionuclides (Baccolo et al., 2017; Łokas et al., 2016, 2018; Owens et al., 2019), with radioecological consequences concerning the presence of FRNs that extend to the proglacial areas (Łokas et al., 2017; Owens et al., 2019). In addition to FRNs, cryoconite has also been shown to accumulate other anthropogenic contaminants including heavy metals (Nagatsuka et al., 2010; Łokas et al., 2016; Baccolo et al., 2017; Singh et al., 2017; Huang et al., 2019), artificial organic compounds (Ferrario et al., 2017; Weiland-Bräuer et al., 2017) and microplastics (Ambrosini et al., 2019). However, among the species found in cryoconite, radionuclides show by far the highest concentration with respect to other environmental matrices. The considerable activity concentrations of artificial FRNs found in cryoconite have allowed for the application of cutting-edge radiological techniques, offering important insight into the sources and distribution of radioactivity deposited within the glaciated regions of the Earth (Łokas et al., 2018, 2019) and making novel contributions to the emerging field of environmental nuclear forensics (Steinhauser, 2019).

Even though the link between cryoconite and environmental radioactivity is now indisputable, several important questions remain. Firstly, it is not clear why and how cryoconite accumulates radionuclides and other anthropogenic impurities and to what extent this accumulation is related to processes specific to glacial environments. Previous studies (Osburn, 1963; Pourcelot et al., 2003) have focused on the role of snowmelt in accumulating radionuclides in residual snow patches during summer, suggesting that nival and melt processes could encourage local accumulation of radioactivity

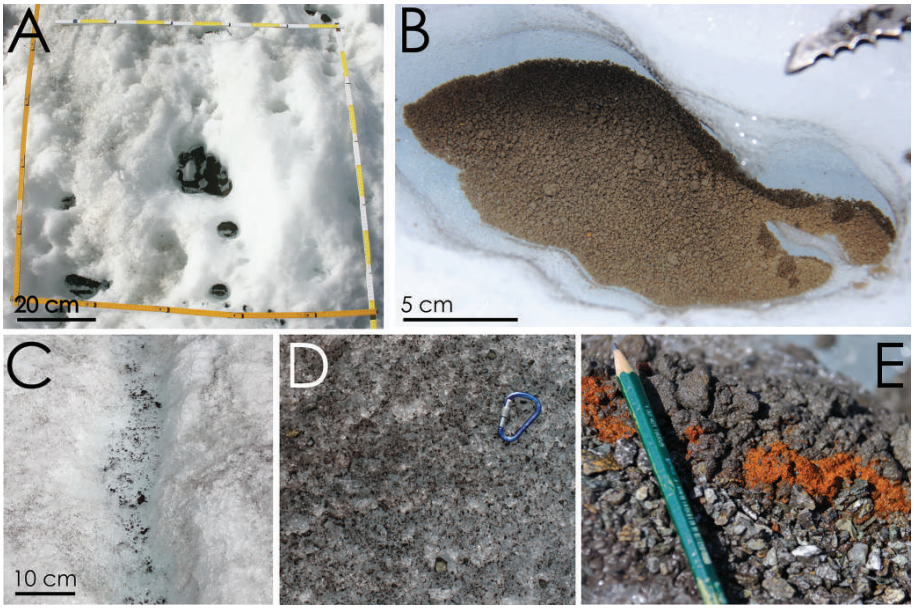

Figure 1. Cryoconite from the Morteratsch **(a)** and Forni **(b)** glaciers. Panel **(c)** shows the beginning of the melt season at the Morteratsch glacier. The ice surface has been exposed to the atmosphere after snow melting, and cryoconite preferentially accumulates within the early meltwater channels. Panel **(d)** shows the end of the melt season at the Morteratsch glacier. The ice surface has experienced months of melting and is now largely covered by cryoconite. Panel **(e)** shows a cryoconite deposit (at the Morteratsch glacier) located few meters downstream from a melting snow patch rich in Saharan dust. Cryoconite aggregates acted as a filter, retaining and accumulating dust particles.

in a similar fashion to what has been observed in cryoconite on glaciers. Secondly, it is not fully understood where this radioactivity comes from.

This paper aims to present cryoconite as a promising tool for radioecological monitoring in high-latitude and high-altitude areas and sheds light on some of the open issues related to the themes explored above. Data concerning cryoconite from two Alpine glaciers are presented and compared to data from previous studies on both cryoconite and other environmental matrices used for radioactive monitoring.

2 Study site and sampling strategy

The Morteratsch and Forni glaciers are located in the European Alps and are situated ~ 50 km apart (Fig. 2). Both glaciers are among the biggest and most studied in the Alps (Azzoni et al., 2017; Di Mauro et al., 2019). The Morteratsch is a Swiss glacier and the largest in the Bernina range, spanning an altitudinal range of roughly 2000 m and with a terminus located at 2100 m a.s.l. It has an area of $\sim 7.5\,km^2$, but until 2015 the value exceeded $15\,km^2$ due to its connection with a tributary glacier that has since detached. A similar setting characterizes the Forni glacier, the biggest one in the Ortles-Cevedale range in Italy. Forni is a north-facing valley glacier presenting a glacial tongue that was, until recently, fed by three accumulation basins. Owing to retreat of the glacier, the connections between the basins have become weaker and the glacier is now fragmented in two parts (Azzoni et al., 2017). The Forni glacier ranges between 2500 and 3750 m a.s.l. and is characterized by a surface area of $\sim 10\,km^2$ considering both ice bodies. From a climatic perspective, the glaciers are similar; they are characterized by a continental climate and in the last years experienced a darkening of their ablation zones because of the accumulation of impurities on the surface and the progressive emergence of detritus from medial and lateral moraines (Di Mauro et al., 2017; Fugazza et al., 2019). The abundance of supraglacial debris is favorable for the formation of cryoconite, and in fact the two glaciers are well studied in terms of cryoconite and its components (Baccolo et al., 2017; Di Mauro et al., 2017; Pittino et al., 2018a; Ambrosini et al., 2019; Fugazza et al., 2019). We have also considered these glaciers because of the relatively easy access, which makes them ideal sites for annual sampling campaigns.

Samples considered here were collected in summer 2015 (July and September) and 2016 (July) from the ablation zones of the glaciers (Fig. 2). Each sample represents a distinct cryoconite hole. The sampling was carried out using sterile disposable pipettes and ethanol-cleaned spoons; samples were kept in sterile tubes at 0 °C during the field campaign and stored at −20 °C in the EUROCOLD laboratory of the University of Milano-Bicocca, until preparation for the geochemical analyses. We selected the most abundant cryoconite deposits, so as to also have material available for other analyses: 12 samples have been gathered on the Morteratsch glacier (between 2100 and 2300 m a.s.l.) and 10 on the

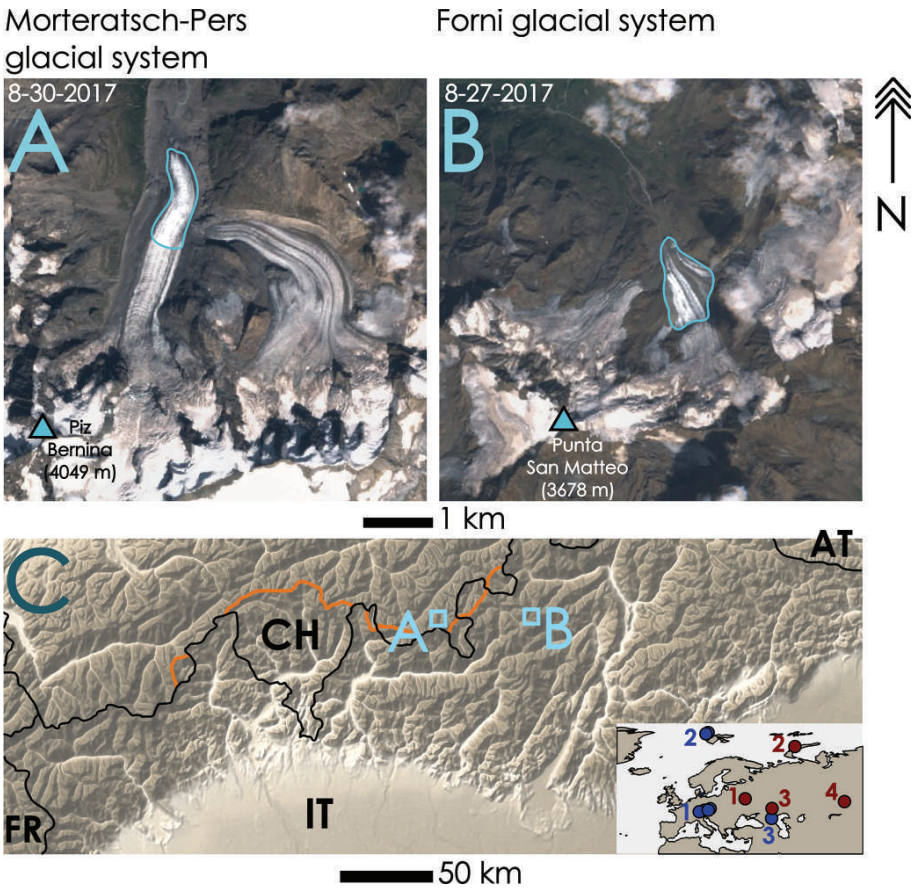

Figure 2. The geographic setting of the present work. Satellite images (ESA Sentinel-2) of the considered glaciers **(a, b)**. The highest peak point within the two catchments is highlighted; the blue lines define the ablation areas where cryoconite has been collected. Panel **(c)** shows a wider view of the central sector of the European Alps. The black line represents national borders, while the orange line, when not coincident with the black one, shows the northern–southern Alpine watershed dividing line. In the box a map shows the sites cited in the discussion: Alpine (1), Svalbard (2) and Caucasus (3) glaciers where cryoconite has been studied from the radiological perspective (blue dots); Chernobyl (Ukraine, 1); Novaya Zemlya (Russia, 2), Semipalatinsk (Kazakhstan, 3) and Kapustin Yar (Russia, 4) nuclear testing areas (red dots).

Forni glacier (between 2600 and 2800 m a.s.l.), each one consisting of 10–40 g of wet cryoconite. Where possible, multiple analyses have been carried out on the same samples, but this has not been always possible. Part of the data concerning gamma spectrometry applied to cryoconite from the Morteratsch samples have already been published (Baccolo et al., 2017).

3 Materials and methods

3.1 Radioactivity measurements

The activity of natural and artificial radionuclides in cryoconite has been measured using a number of techniques. ^{137}Cs, ^{241}Am, ^{207}Bi, ^{40}K, and ^{238}U and ^{232}Th decay chain nuclides were analyzed through γ-spectrometry about 6 months after sampling; full details are found in the Supplement. Aliquots dedicated to γ-spectrometry consist of $\sim$ 1 g of dry material (dried until constant weight at 50 °C, 2 mm sieved) sealed in polyethylene vials. The acquisition of the γ-spectra took place at least 2 weeks after the sealing, to allow the secular equilibrium between ^{222}Rn and its progenies to be attained. Each sample has been counted for 1 week using a customized high-purity germanium well detector (Ortec). Details about the instrument, calibration and analytical performances are presented elsewhere (Baccolo et al., 2017). Aliquots dedicated to Pu analyses ($\sim$ 1 g of dry material) have been ashed at 600 °C to remove organic matter. The ash has been dissolved with mineral acids and the resultant liquid samples have undergone radiochemical separation and concentration of Pu. The procedure is extensively described elsewhere by Łokas et al. (2016). Activities of $^{239+240}$Pu and ^{238}Pu have been determined through α-spectrometry after Pu co-precipitation with NdF_3 using Canberra 7401 and Ortec Alpha Duo spectrometers. After further radiochemical purification, the ^{240}Pu/^{239}Pu atomic ratio was measured through multicollector inductively coupled mass spectrometry (MC-

ICP-MS) (Thermo Fisher Scientific Neptune spectrometer), in accordance with Łokas et al. (2018). ^{238}U and ^{232}Th activities have not been directly measured but have been estimated considering the total content of U and Th.

3.2 Instrumental neutron activation analysis

The Th and U composition of cryoconite was assessed through instrumental neutron activation. Samples were irradiated at the LENA laboratory, where a TRIGA Mark II nuclear reactor is available. The irradiation lasted for 6 h under a thermal neutron flux of $2.4 \pm 0.2 \times 10^{12}$ neutron s^{-1} cm^{-2}. To determine the concentration of Th and U in the samples, the following nuclear reactions and γ-emissions were exploited: ^{232}Th (n, γ) ^{233}Th $\rightarrow$ ^{233}Pa (analyzed emissions: 300.3 and 312.2 keV) and ^{238}U (n, γ) ^{239}U $\rightarrow$ ^{239}Np (analyzed emissions: 228.2 and 277.6 keV). Irradiated samples were counted for 6 h a few days after the irradiation, using the same well detector applied for γ-spectrometry. The quantification of concentrations was carried out comparing samples and reference materials (Baccolo et al., 2017).

3.3 Carbonaceous content

A thermo-optical analyzer (Sunset Lab Inc. analyzer) has been used for the determination of organic and elemental carbon content (OC and EC, respectively), following the protocol adopted in Baccolo et al. (2017). Cryoconite samples have been suspended on clean quartz fiber filters and analyzed. The mass concentration of OC and EC has been obtained combining the information relative to filter superficial concentrations and the mass of cryoconite deposited on the latter, determined using an analytical microbalance (precision 1 µg) which has been operated inside an air-conditioned room ($T = 20 \pm 1$ °C; relative humidity $= 50 \pm 5$ %). Mass concentration of OC has been converted into organic matter content (Pribyl, 2010).

3.4 Statistics

To evaluate the degree of correlation between variables and samples, two multivariate statistical tools have been applied. Multidimensional scaling (MDS) has been used to appreciate the degree of correlation between the radionuclides (Diaconis et al., 2008). MDS has been applied to a similarity metric derived from the correlation matrix (Pearson's correlation coefficient) of the original data, following Eq. (1), where the distance d between variables v_1 and v_2 is obtained considering their Pearson correlation coefficient (r) (van Dongen and Enright, 2012).

$$d(v_1, v_2) = \sqrt{1 - r(v_1, v_2)^2} \quad (1)$$

The correlation between samples and the differences between the two glaciers have been evaluated applying the principal component analysis (PCA) method to standardized data. The first two components (which explain 65 % of the total variance) have been taken into consideration.

4 Results and discussion

4.1 Cryoconite natural radioactivity

Our results confirm the ability of cryoconite to accumulate radioactivity and in particular FRNs. In fact only FRNs, whose environmental occurrence is related to atmospheric transport, are actually accumulated in cryoconite from the Morteratsch and Forni glaciers, not the lithogenic ones. This can be observed in Fig. 3, where the activity of lithogenic radionuclides is presented. A substantial secular equilibrium characterizes the nuclide belonging to the ^{238}U and ^{232}Th decay chains, except for ^{210}Pb ($t_{1/2} = 22.3$ years), which presents an excess with respect to the other ^{238}U-related nuclides. Excluding it, the average ^{238}U and ^{232}Th chain activities are 70 ± 15 and 52 ± 8 Bq kg^{-1}, respectively, for the ^{238}U chain (Morteratsch and Forni samples, $\pm$ standard deviation) and 50 ± 10 and 55 ± 10 Bq kg^{-1} for the ^{232}Th chain. These values, as seen in Fig. 3, are slightly higher than the average ^{238}U and ^{232}Th radioactivity of upper continental crust (UCC) reference (Rudnick and Gao, 2003), which is 34 and 43 Bq kg^{-1} for ^{238}U and ^{232}Th, respectively. The difference is probably related to the accumulation in cryoconite of heavy minerals, where U and Th are typically enriched, because of hydraulic sorting related to meltwater flow (Baccolo et al., 2017). The activity of the primordial radioactive nuclide ^{40}K ($t_{1/2} = 1.28 \times 10^9$ years) in the samples from the Morteratsch and Forni glaciers (810 ± 55, 770 ± 200 Bq kg^{-1}) is of the same order of magnitude as ^{40}K UCC activity, i.e., 720 Bq kg^{-1} (Rudnick and Gao, 2003). Such results point to a typical crustal origin for the lithogenic radionuclides measured in cryoconite. An exception to this is ^{210}Pb, which, although being a decay product of ^{238}U progeny, shows activity levels 2 orders of magnitude higher than the other ^{238}U-chain nuclides. The average activities in the samples from the Morteratsch and Forni glaciers are 2800 ± 800 and 6200 ± 1900 Bq kg^{-1}, respectively, and are statistically different (Student's t test: $t_{20} = 5.9$; p value < 0.001) within the two glaciers. Finding such high ^{210}Pb activities in samples collected on the surface of glaciers is not completely unexpected. It is common to observe an excess of ^{210}Pb in Earth surface environments, due to its dual source. A fraction of ^{210}Pb is present in materials of geologic origin because of the internal decay of ^{238}U progeny (supported ^{210}Pb); a second fraction (unsupported ^{210}Pb) is found in samples exposed to the atmosphere and is attributable to the scavenging by precipitation of atmospheric ^{210}Pb, produced from the decay of the gaseous ^{222}Rn released into the atmosphere from rocks and soils. Given its relatively long half-life (22.3 years), precipitated ^{210}Pb concentrates in surficial environments, but typically its activity does not exceed tens or a few hundred of

becquerels per kilogram in matrices strongly influenced by atmospheric deposition and rich in organic matter, for which Pb shows a particular affinity (Strawn and Spark, 2000).

In Fig. 4, cryoconite radioactivity is compared to data concerning other environmental matrices. With respect to lichens and mosses, which are known to be efficient in accumulating radioactive atmospheric species (Kirchner and Daillant, 2002), cryoconite shows a ^{210}Pb activity that is, on average, higher by 1 order of magnitude. Two hypotheses are made to explain the excess found in cryoconite: (1) the glaciers considered here are located in areas where the atmospheric deposition of ^{210}Pb is enhanced; (2) cryoconite is more efficient at concentrating atmospherically derived radionuclides than lichens and mosses. At the Morteratsch glacier a comparison has been made between cryoconite and samples collected from the surface of the moraines surrounding the glacier (Baccolo et al., 2017). The moraine sediments have had a mean activity of $145 \pm 30\,\mathrm{Bq\,kg^{-1}}$ for unsupported ^{210}Pb, while in cryoconite it has exceeded $2500\,\mathrm{Bq\,kg^{-1}}$. This evidence rejects the first hypothesis: if an anomaly of atmospheric ^{210}Pb deposition was present in the Morteratsch valley, it should impact both the moraine and glacial surfaces. Several studies have reported high unsupported ^{210}Pb activity in cryoconite from different regions of the Earth (Tieber et al., 2009; Baccolo et al., 2017; Łokas et al., 2016, 2018), suggesting that high ^{210}Pb activity is related to specific characteristics of cryoconite.

4.2 Anthropogenic radioactivity in cryoconite and other environmental matrices

In Fig. 4, the comparison between radioactive contamination of worldwide lichens, mosses, soils and sediments from other studies (full information in the Supplement) is extended to all of the radionuclides that have been found in excess in cryoconite in this study. Out of all of them, ^{210}Pb is the only natural occurring species while the others are anthropogenic in origin. In descending order of average activity in cryoconite, they are ^{137}Cs ($t_{1/2} = 30.1$ years), $^{239+240}$Pu ($t_{1/2} = 24\,110$ and 6536 years, respectively), ^{241}Am ($t_{1/2} = 432.2$ years), ^{207}Bi ($t_{1/2} = 31.6$ years) and ^{238}Pu ($t_{1/2} = 87.7$ years). These nuclides have been released into the environment as a consequence of nuclear incidents and explosions and have been atmospherically transported and deposited globally. For all radionuclides, the activities measured in cryoconite are always higher than those of other environmental matrices (see Fig. 4). To find samples with activities comparable to the ones found in cryoconite, it would be necessary to consider sites within the vicinity of nuclear tests or incidents. The mean ratios between the activity levels found in cryoconite and in lichens for ^{137}Cs, $^{239+240}$Pu, ^{241}Am, ^{207}Bi and ^{238}Pu are 9.5, 58, 39, 35 and 7, respectively, and the values are even higher when matrices less efficient in accumulating radionuclides are considered. This supports the hypothesis that cryoconite accumulates atmospherically derived artificial radionuclides more efficiently than other matrices, as already suggested by exploring unsupported ^{210}Pb.

The accumulation ability of cryoconite can be observed not only for common artificial radionuclides, such as ^{137}Cs and ^{239,240}Pu, but also for less abundant species, such as ^{241}Am, ^{207}Bi and ^{238}Pu. ^{137}Cs is among the most common long- lived fission products from ^{235}U and has been released in the environment due to commercial reactor failures and fission bomb test explosions. The plutonium isotopes 239 and 240 also originate from atmospheric weapon tests and nuclear accidents, but the relative contribution from atmospheric tests is larger, since ^{239}Pu has been the most common fissile material used in fission bombs and for igniting fusion devices. Because of their widespread dispersion, ^{137}Cs and ^{239,240}Pu are the most abundant artificial nuclides found in cryoconite from the two glaciers, confirming previous results (Tieber et al., 2009; Łokas et al., 2018, 2019). Their mean activities in the samples from Morteratsch and Forni glaciers are 2600 ± 3800 and $1900 \pm 2900\,\mathrm{Bq\,kg^{-1}}$ for ^{137}Cs and 80 ± 75 and $4.9 \pm 0.9\,\mathrm{Bq\,kg^{-1}}$ for ^{239,240}Pu (average activities and standard deviations for the Morteratsch and Forni cryoconite, respectively). Less abundant nuclides are present in cryoconite with lower concentration, including ^{241}Am (30 ± 35 and $4 \pm 1.5\,\mathrm{Bq\,kg^{-1}}$), ^{207}Bi ($9 \pm 7$ and $6 \pm 2\,\mathrm{Bq\,kg^{-1}}$) and ^{238}Pu ($2.5 \pm 2.5$ and $0.22 \pm 0.08\,\mathrm{Bq\,kg^{-1}}$). Despite being low, such activities are still significant and among the highest ever found in the environment. Typical environmental activities usually do not exceed $1\,\mathrm{Bq\,kg^{-1}}$ for ^{241}Am and ^{207}Bi and $0.1\,\mathrm{Bq\,kg^{-1}}$ for ^{238}Pu (Fig. 4), with their rarity being related to their production mechanisms (Shabana and Al-Shammari, 2001; Bossew et al., 2006). The presence of ^{241}Am in the environment is not primarily related to direct deposition (it is present in nuclear power plant spent fuel); it is mostly produced in situ, from the decay of its parent nuclide (^{241}Pu, $t_{1/2} = 14.3$ years), which has been released into the environment alongside other Pu isotopes. Thanks to ^{241}Pu decay, the environmental activity of ^{241}Am globally is increasing and will peak around the year 2100 (Thakur and Ward, 2018). ^{238}Pu is one of the rarest plutonium isotopes produced by commercial reactors and nuclear explosions, and its diffusion is mostly related to the atmospheric reentry of satellites powered by pure ^{238}Pu thermoelectric generators (Łokas et al., 2019) and to a smaller degree by the release from nuclear fuel reprocessing plants into the marine environment (Bryan et al., 2008). ^{207}Bi has been released as a consequence of a few high-yield thermonuclear explosion tests (Noshkin et al., 2001) and has rarely been observed within the environment. Finding easily detectable activities in cryoconite for these rare radionuclides, many of which were released decades ago, is both surprising and unprecedented. Studies focused on them usually require the application of preconcentration and separation procedures, but for cryoconite a direct measure of activity was sufficient. These results highlight the po-

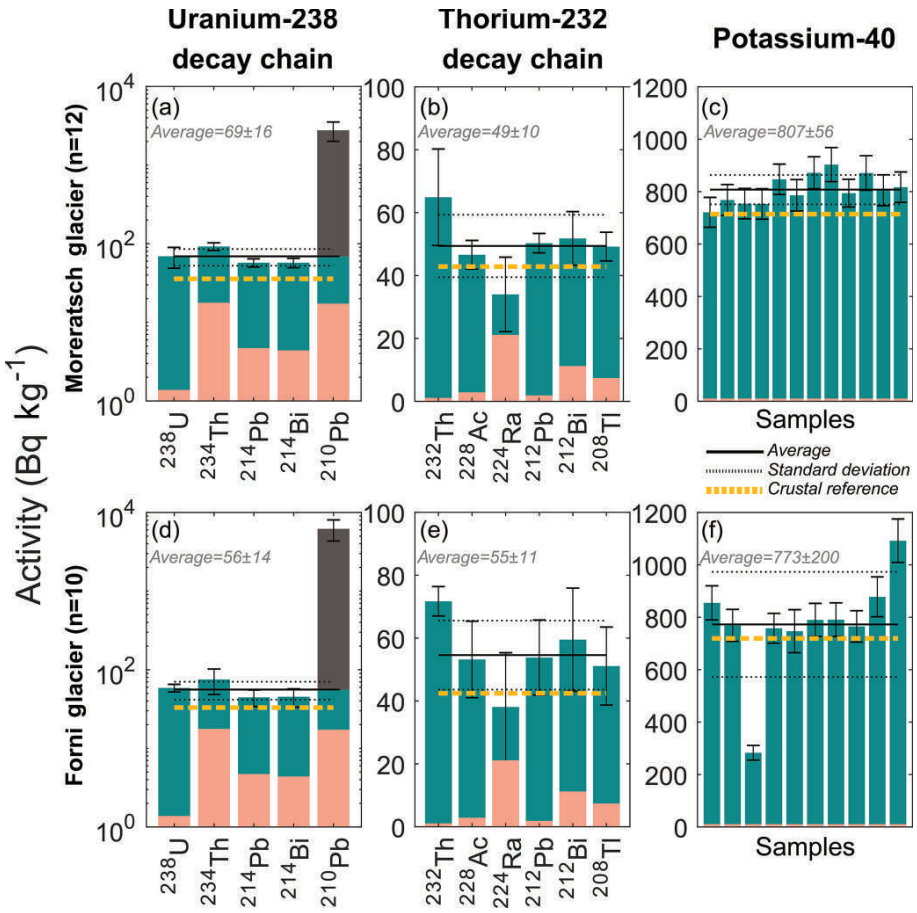

Figure 3. Activity of the radionuclides belonging to the decay chains of ^{238}U and ^{232}Th and of ^{40}K. Panels **(a)**, **(b)** and **(c)** refer to cryoconite from the Morteratsch glacier and panels **(d)**, **(e)** and **(f)** to cryoconite from the Forni glacier. Red bars represent detection limits and green bars measured activities. The activity of ^{210}Pb is divided into supported (green bar) and unsupported fractions (grey bar), considering the upper ^{238}U decay chain as reference for the supported fraction. Crustal references are calculated from Rudnick and Gao (2003).

tential of this environmental matrix for radioecological monitoring.

Looking in detail at the two Alpine glaciers considered here, only the activity of Pu isotopes is significantly different between the two sites, with higher values found in the samples from the Morteratsch glacier (Student's t test: $t_{12} = 2.99$; p value $= 0.010$ for both ^{238}Pu and $^{239+240}$Pu). ^{241}Am is also more abundant in Morteratsch cryoconite, but not significantly because of the large standard deviation (Student's t test: $t_{20} = 2.24$; p value $= 0.018$). The ratios between the mean activity of the Morteratsch and Forni samples are 15.9, 11.6 and 6.8 for $^{239+240}$Pu, ^{238}Pu and ^{241}Am, respectively.

4.3 Sources of anthropogenic radioactivity in cryoconite

To infer the potential sources of the radioactivity found in cryoconite from Alpine glaciers, isotopic and activity ratios between Pu and Cs isotopes have been calculated (Fig. 5). The use of such ratios has been to estimate the provenance of environmental radioactivity, since specific signatures are associated with different sources (Steinhauser, 2019). The atomic ratio ^{240}Pu/^{239}Pu and activity ratio ^{238}Pu/$^{239+240}$Pu show that the plutonium-related radioactivity of Morteratsch and Forni cryoconite is compatible with the worldwide signal from global radioactive fallout (Table 1 and Fig. 5a, b). The latter reflects the composition of the stratospheric reservoir, established in the 1960s as a consequence of atmospheric nuclear weapon testing. On average, more than 99 % of the Pu found in cryoconite from the Morteratsch glacier is from global fallout, while for the Forni glacier the average contribution is 95 %, suggesting a non-negligible influence from the Chernobyl accident ($\sim$ 5 %).

By comparing the ^{240}Pu/^{239}Pu ratio of global fallout and of modern snow deposited in the Alps (Gückel et al., 2017), it is possible to further discuss the Pu sources in cryoconite. Modern Alpine snow has a slightly higher ratio than global fallout (0.21 vs. 0.18), probably because of the partial influence of resuspended Chernobyl radioactive fallout, which

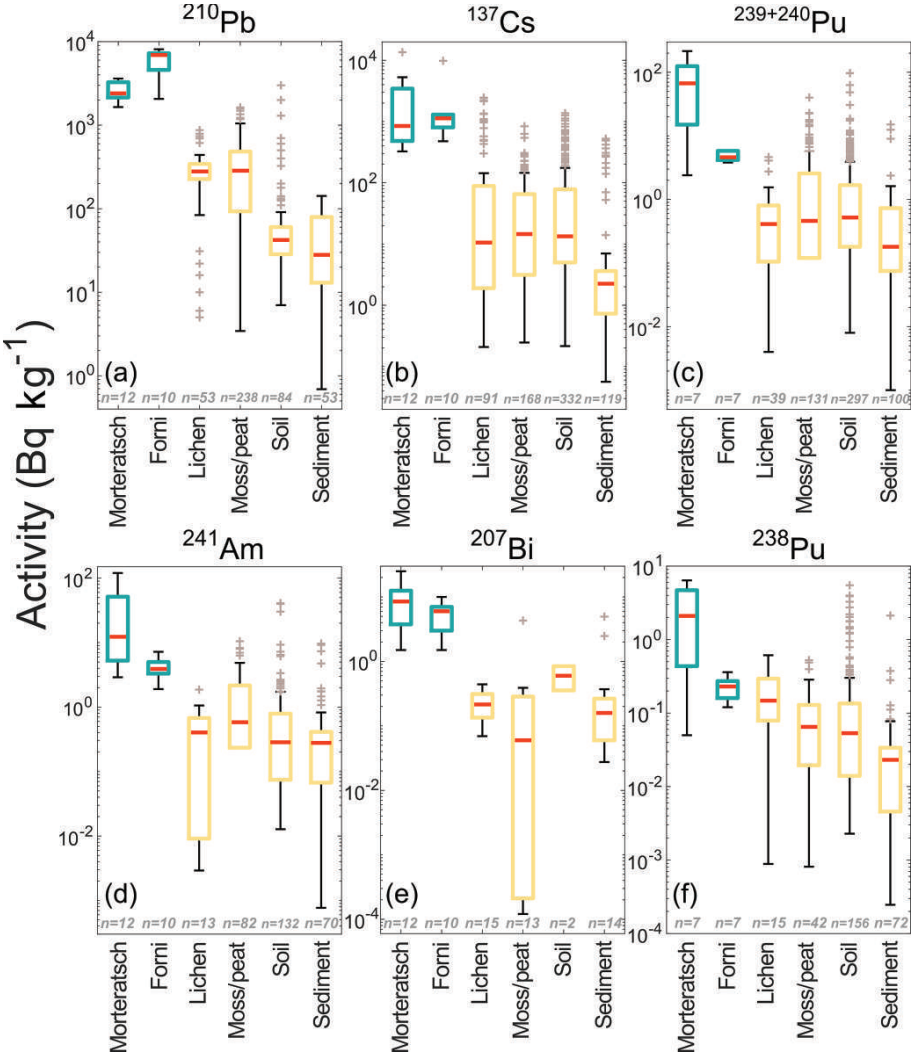

Figure 4. Radionuclides presenting anomalously high activities in cryoconite compared to other environmental matrices. Activity in cryoconite (green boxes) is compared to data from literature concerning the contamination in other matrices sampled in surficial environments (yellow boxes). The number of considered samples is shown in the lower part of each plot. Given the number of publications from which the displayed data were sourced, they have been listed individually in the Supplement. All activities were corrected for decay at June 2017, with the exception of ^{210}Pb, which, being continuously produced in the atmosphere, did not require any adjustment.

is more enriched in ^{240}Pu than global fallout (Ketterer and Szechenyi, 2008). Only two cryoconite samples (one from Forni and one from Morteratsch) show a Pu isotopic composition pointing to the Chernobyl influence. They show a ratio of 0.286 ± 0.006 and 0.24 ± 0.02, respectively, which is even higher than that of modern Alpine snow. The occurrence of only two samples with a partial Chernobyl signature can be explained by the presence of fallout particles from Chernobyl nuclear fuel in these specimens. The non-volatile constituents of nuclear fuel, such as Pu, were not scattered into the environment homogenously, as in the case of the more volatile ^{137}Cs, but as micrometric and highly radioactive particles (Sandalls et al., 1993). The presence of even one of such particles in the two samples could be sufficient to explain the anomalies. The other samples present a global signature fully compatible with global fallout and not with modern Alpine snow. This implies that Pu accumulated in Alpine cryoconite dates back to when the deposition of radionuclides was dominated by global stratospheric fallout, approximately from 1960 to 1980 (Hirose et al., 2008). The deposition of plutonium, which is still occurring on the Alpine snowpack, is too weak to influence the isotopic fingerprint of cryoconite. Pu activity in fresh snow ranges from 0.4 to 11.5 μBq kg^{-1} (Gückel et al., 2017), roughly 6 orders of magnitude lower than the average activity of cryoconite, which is 41 Bq kg^{-1}. This has important implications because it suggests that cryoconite is more influenced by past atmospheric fallout rather than contemporary fallout,

Table 1. Data about the fraction of Pu and ^{137}Cs related to global fallout in cryoconite samples from the Morteratsch and Forni glaciers and from other glaciers. To calculate global fractions, reference ratios defined by Ketterer et al. (2008), Cagno et al. (2014), Gückel et al. (2017) and Wilflinger et al. (2018) have been used.

Glacier (sample nr.)	Geographical location	Pu from global fallout (%)	^{137}Cs from global fallout (%)
Morteratsch (7) this study	Alps	99 ± 2	41 ± 18
Forni (6) this study	Alps	95 ± 3	12 ± 6
Stubacher Sonnblickkees (19) Tieber et al. (2009)	Alps	n.a.	5 ± 4
Hallstätter (8) Wilflinger et al. (2018)	Alps	n.a.	10 ± 8
Adishi (8) Łokas et al. (2018)	Caucasus	99 ± 2	36 ± 19
Waldemarbreen (9) Łokas et al. (2019)	Svalbard	93 ± 4	56 ± 25

at least when considering Pu. The only source that can provide cryoconite FRNs from past atmospheric deposition is ice accumulated within the period of maximum deposition of atmospheric radioactivity, when it was dominated by global stratospheric fallout. The presence of ^{207}Bi in cryoconite also supports this hypothesis. In the Northern Hemisphere ^{207}Bi was produced during the explosion of the Tzar thermonuclear device in 1961 in Novaya Zemlya (Aarkrog and Dahlgaard, 1984). A few years after this event the ^{207}Bi atmospheric contamination decreased until reaching undetectable levels (Kim et al., 1997). If a considerable amount of ^{207}Bi is present in cryoconite, it means that the cryoconite has had the possibility to interact with ice deposited shortly after 1961.

Comparing our results with the data obtained for cryoconite collected in the Caucasus and in regions of the Arctic (Łokas et al., 2018, 2019), it is possible to see that there are variations in the radioactive signatures, pointing to secondary regional influences, despite the fact that the general features are compatible with global stratospheric fallout (Fig. 5). Caucasian and Arctic samples are characterized by a lower ^{240}Pu/^{239}Pu atomic ratio than the Alpine samples (Fig. 5a and b). Such a signature is compatible with the influence of weapon-grade Pu, depleted in ^{240}Pu (Cagno et al., 2014). It has been argued that samples from the Caucasus were influenced by the debris spread from the Semipalatinsk (Kazakhstan) and Kapustin Yar (Russia) test sites, where hundreds of nuclear explosions have been carried out (Łokas et al., 2018). The effects of high-latitude nuclear polygons (Novaya Zemlya) and of the reentry of ^{238}Pu-powered satellites explain the non-global fallout contribution observed in the Arctic cryoconite, which is enriched in both ^{239}Pu and ^{238}Pu with respect to the Morteratsch and Forni samples (Łokas et al., 2019). The latter, showing a good agreement with the global fallout reference, rule out the possibility that a fraction of the Pu found in Alpine cryoconite was produced during the Algerian atmospheric nuclear tests carried out by France in the 1960s.

By studying the ^{137}Cs and $^{239+249}$Pu activity ratio (Table 1 and Fig. 5c), it is possible to infer the potential sources of ^{137}Cs, whose activity is by far the highest among the artificial radionuclides found in cryoconite. While global fallout has been demonstrated as the main source of Pu, the same is not true for ^{137}Cs. On average, the ^{137}Cs fraction found in the Morteratsch glacier samples from global fallout is 41 % with respect to total ^{137}Cs. For the Forni samples the value is lower (12 %). The non-global fraction of ^{137}Cs found in Alpine cryoconite is attributable to the radioactive contamination released during the Chernobyl event. The Alps, and in particular the eastern Alps, were among the most heavily impacted areas by Chernobyl fallout, where ^{137}Cs was a dominant component (Steinhauser et al., 2014). This is confirmed by the radioactive signature of cryoconite from two Austrian Alpine glaciers in the eastern Alps (Tieber et al., 2009; Wilflinger et al., 2018), whose ^{137}Cs content is dominated by Chernobyl contamination (more than 90 %). Samples from the Caucasus also show a dominant Chernobyl contribution with respect to ^{137}Cs, while cryoconite from Svalbard is anomalous in being characterized by a primary influence from global fallout (56 %). This is, however, not unexpected since, among the glaciers considered in Fig. 5, Waldemarbreen (Svalbard) is the farthest from Chernobyl.

While Pu has a dominant global source, ^{137}Cs is related to both global and Chernobyl-related fallouts. Pu, together with the other actinides, is highly non-volatile, and its trans-

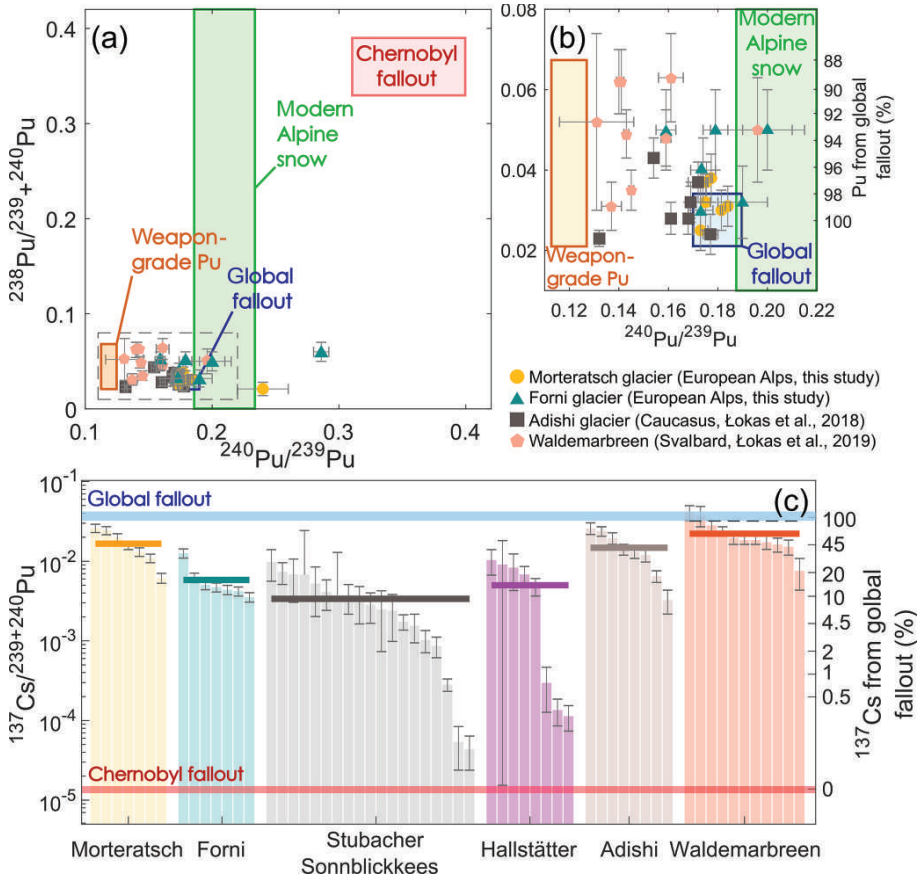

Figure 5. The fingerprint of cryoconite radioactivity. **(a, b)** Pu isotopic composition of cryoconite samples (panel **b** is an enlargement of panel **a**). $^{238}Pu/^{239+240}Pu$ is expressed as an activity ratio, ^{240}Pu to ^{239}Pu as an atomic ratio. **(c)** ^{137}Cs-to-$^{239+240}Pu$ activity ratio of cryoconite. In addition to the Forni and Morteratsch glacier samples, data from the Austrian Alps (Stubacher Sonnblickkees and Hallstätter glaciers; Tieber et al., 2009; Wilflinger et al., 2018), Svalbard (Waldemarbreen; Łokas et al., 2019) and from the Caucasus (Adishi glacier; Łokas et al., 2018) are included. Reference ratios (blue square for global fallout, red square for Chernobyl fallout, yellow square for weapon-grade Pu, green square for modern Alpine snow) are from literature (Ketterer et al., 2008; Cagno et al., 2014; Gückel et al., 2017; Wilflinger et al., 2018). All values are corrected for decay to June 2017. A geographic setting of the data presented here is found in Fig. 2.

port mostly takes place through the dispersion of micrometric particles from nuclear fuel, fission and activation products (Sandalls et al., 1993), while Cs is volatile and its mobilization during nuclear accidents requires relatively low temperatures. The Pu contamination from Chernobyl was limited to a few hundreds of kilometers from the emission site and could not be efficiently transported for long distances, while ^{137}Cs transport was widespread, leaving a strong signature all over Europe (Steinhauser et al., 2014), as is also supported by Alpine cryoconite.

4.4 Carbonaceous content

Results of carbon analyses are presented in Fig. 6. On average (± standard deviation), the carbonaceous composition of the Morteratsch glacier samples is 9.4 ± 1.4 % mass ratio for organic matter and 0.50 ± 0.25 % mass ratio for elemental carbon. Cryoconite from the Forni glacier contains a lower concentration of both species: 7.2 ± 0.8 % for organic matter and 0.2 ± 0.2 % for elemental carbon. Values for organic matter are compatible with the wider literature, where organic matter in cryoconite has been reported to vary between 2 and 18 % (Cook et al., 2015). Very limited information is available about the elemental and/or black carbon composition of cryoconite, despite a great deal of attention having been given to the carbonaceous impurities present in snow in relation to the effect on ice and snow darkening (Di Mauro et al., 2017). Our results show that elemental carbon is accumulated in cryoconite with respect to Alpine snow, where typical concentrations are orders of magnitude lower (Jenk et al., 2006). Only contaminated urban soils present an elemental carbon concentration comparable to Alpine cryoconite samples (Lorenz et al., 2006). These findings support the hypotheses by Hodson (2014), who has suggested that cryoconite plays a role in extending the residence time of black and elemental carbon on the surface of glaciers, with

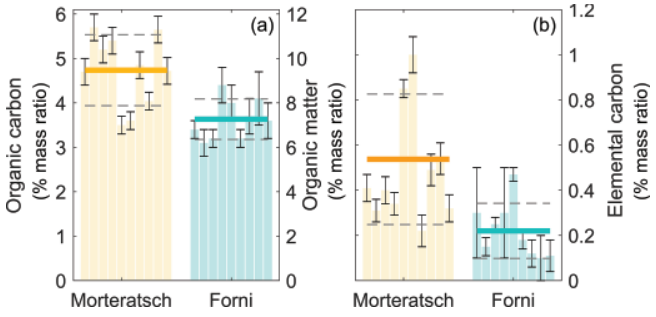

Figure 6. Carbonaceous content of Alpine cryoconite: organic carbon (and estimated organic matter) is shown in panel **(a)**, elemental carbon in panel **(b)**. Mean values are depicted alongside standard deviations (colored and dashed lines).

implications for the accumulation of hydrophobic contaminants and for ice darkening.

Cryoconite from the Morteratsch glacier presents a higher concentration of both organic and elemental carbon than that from the Forni glacier (Student's t test: $t_{19} = 3.80$; p value < 0.001 for organic carbon concentration; Student's t test $t_{19} = 3.10$; p value $= 0.003$ for elemental carbon). We hypothesize that elevation has a role in explaining the difference. Cryoconite from the Morteratsch glacier has been sampled at an elevation between 2100 and 2300 m a.s.l., while samples from the Forni glacier have been collected between 2600 and 2800 m a.s.l. A higher elevation implies lower temperatures, a shorter summer season and thus a less pronounced biochemical activity, which is in accordance with the lower organic carbon content observed in cryoconite at the Forni glacier.

4.5 Considering radioactivity as a whole

To analyze possible relationships between the different radionuclides, MDS and PCA have been applied to our data. The first tool has been used to represent the degree of similarity and dissimilarity between the radionuclides (Fig. 7a). In the two-dimensional domain of MDS, the radionuclides are grouped within three clusters which are interpreted as (1) artificial radionuclides, (2) ^{238}U-chain nuclides and (3) ^{232}Th-chain nuclides. Despite ^{40}K not belonging to any of these groups, its distance from the ^{238}U and ^{232}Th chain clusters is limited, confirming that K, Th and U in cryoconite are all associated with lithogenic components. The most isolated of the nuclides is unsupported ^{210}Pb, in accordance with its peculiar biogeochemical cycle.

MDS is able to highlight the different sources of the radionuclides considered in this study: (1) the artificial radionuclides, whose presence on glaciers is mostly related to stratospheric fallout, (2) the lithogenic radionuclides which are present in the mineral fraction of cryoconite and (3) ^{210}Pb which is deposited onto the glacier from the lower troposphere by precipitation. This partitioning is useful for interpreting the differences observed between the two glaciers considered here. At the Morteratsch glacier the activity of the stratospherically derived radionuclides (Pu, Am, Bi) is higher than on Forni glacier; for ^{210}Pb the opposite is true (Fig. 4 and Supplement). This pattern may be related to the altitude of the glaciers. The Morteratsch glacier basin has a maximum altitude of 4049 m a.s.l. and an average elevation higher than 3000 m a.s.l., while the Forni basin is delimited by peaks whose maximum altitude spans from 3200 to 3400 m a.s.l. and only occasionally exceeds 3500 m a.s.l. The lower altitude could explain the higher amount of ^{210}Pb found in cryoconite from the Forni glacier, since the maximum atmospheric scavenging of ^{210}Pb occurs in the lower troposphere, below 4000 m (Guelle et al., 1998). In contrast, the Morteratsch basin, given its high elevation, is more exposed to stratospheric fallout, perhaps explaining why the cryoconite from this glacier is highly contaminated with Pu isotopes, ^{241}Am and ^{207}Bi. Another factor that should be considered to explain the stronger contamination of cryoconite from Morteratsch is the higher concentration of carbonaceous compounds in cryoconite from this glacier, for which radionuclides show a particular affinity (Gadd, 1996; Fowler et al., 2010; Kim et al., 2011; Chuang et al., 2015).

Results from PCA allow for the distinction of cryoconite sampled from the two glaciers. As seen in Fig. 7b–c, the first two components, mostly the second one, separate the Morteratsch and Forni samples. The nuclides diagnostic for the separation in PC2 are the anthropogenic ones, which define the negative scores of Morteratsch samples, and unsupported ^{210}Pb, which is linked to the positive scores of Forni cryoconite. One sample from the Forni glacier is an outlier with respect to the others, being characterized by low concentration activity for most of the radionuclides, in particular the artificial ones.

4.6 The age of cryoconite and its relationship with ice surface processes

Natural and artificial FRNs are widely used to constrain chronologies in sedimentary environments. Among the nuclides considered here, ^{210}Pb and ^{137}Cs are commonly applied for dating, while ^{207}Bi and ^{241}Am have been rarely used to mark the period of maximum FRN deposition from atmospheric weapon tests (Kim et al., 1997; Appleby, 2008). Given the high concentration of radionuclides in cryoconite, it would be interesting to assess if they could be used to estimate the age of cryoconite itself. The most important issue that makes any attempt at dating challenging is the complete absence of a stratigraphic record in cryoconite. In studying cryoconite it is only possible to obtain a set of distinct and uncorrelated samples. Wilflinger et al. (2018) used ^{210}Pb to infer the mixing age (intended as an approximate mean age) of cryoconite samples from an Austrian glacier, the Stubacher Sonnblickkees. To attempt the dating, an assumption was made: once cryoconite is formed, its radioac-

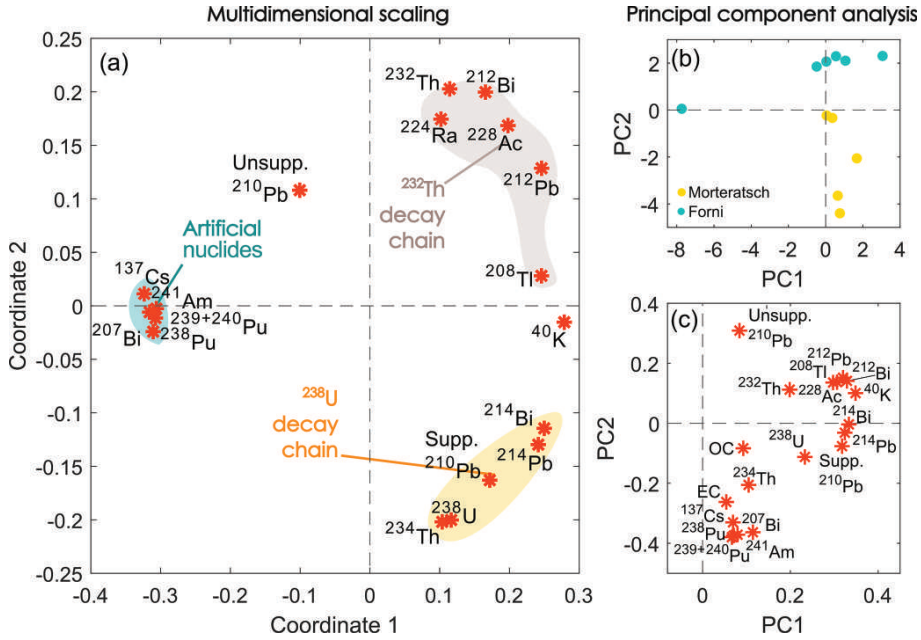

Figure 7. Multivariate statistical analysis applied to Alpine cryoconite radioactivity data. Panel **(a)** results from multidimensional scaling. Panels **(b)** and **(c)** refer to scores and loadings of the first two principal components, respectively, calculated through principal component analysis. OC is organic carbon; EC is elemental carbon.

tive content starts decreasing following the decay law, regardless of the aggregation and dissolution processes that affect cryoconite granules (Takeuchi et al., 2001). Based on this hypothesis, cryoconite is viewed as a sort of pure concentrated airborne material which is rich in atmosphere-derived contaminants, such as FRNs, and maintains its composition despite the dynamism of the supraglacial environment. In Wilflinger et al. (2018) a highly radioactive sample of airborne sediments extracted from fresh snow was interpreted as a sort of time-zero reference (a primordial cryoconite material); however no further details were given about this specimen. Comparing the ^{210}Pb activity of cryoconite to the reference, the mixing age of the samples has been thus inferred. According to this conceptual model, older cryoconite presents lower ^{210}Pb activity in the light of the fact that the more time that has passed from its formation, the more profound ^{210}Pb depletion due to the exponential radioactive decay should be. The estimated ages ranged from a few years to more than a century (Wilflinger et al., 2018). The glacier considered by Wilflinger et al. (2018) is small (less than 1 km^2) and is undergoing significant retreat and fragmentation (Kaufmann et al., 2013). The distribution of cryoconite on glaciers is extremely dynamic and is influenced by meteorological processes, local ice morphology, and supraglacial melting and runoff. It has been observed that within only a few days, single cryoconite holes can form, deepen and collapse, scattering cryoconite granules downstream on the glacier (Takeuchi et al., 2018). In addition, it is known that cryoconite is far from being a static sediment: its granules are in fact subjected to uninterrupted changes, such as aggregation and breakup, and their lifetime on glaciers does not exceed a few years (Takeuchi et al., 2010). In Antarctica, where cryoconite holes are usually covered by a permanent ice lid and supraglacial hydrology is poor, the isolation age (i.e., the time period during which a single cryoconite hole has remained isolated from glacial hydrology) of single cryoconite holes has been estimated through a biogeochemical method: it never exceeds a few years (Fountain et al., 2004; Bagshaw et al., 2007). The transience of surficial glacial environments is further confirmed by glacier moss balls (conglomerations of mineral debris, moss and organic matter forming on the surface of glaciers), whose lifespan was observed not to exceed a few years (Hotaling et al., 2019). Given this evidence, we find it unlikely that a fraction of cryoconite sampled on the surface of a small and steep glacier such as the Stubacher Sonnblickkees could form at the end of the 19th century and persist there since then without being subjected to significant compositional changes.

We present an alternative hypothesis to link the content of FRNs in cryoconite and its formation age. Our conceptual model arises from an assumption opposite to that of Wilflinger et al. (2018): cryoconite is not a static material; its composition changes with time because of the processes taking place on the surface of glaciers. In light of this, the radioactive content of cryoconite is not only subjected to decay, but also to a buildup derived from continuous accumulation. Consequently, the older the cryoconite is, the higher its ^{210}Pb content is, because it has had a longer time within

which to accumulate the radionuclide, which is continuously deposited on the glacier with snow and rain. We hypothesize that the buildup of radioactivity in cryoconite is derived from the interaction between ice, meltwater and cryoconite granules. During summer, the radionuclide content of ice and snow is mobilized through melting, including unsupported ^{210}Pb, which is always present in relatively recent ice (given its lifetime, it is not present at detectable concentrations in ice older than 150–200 years). The interaction between cryoconite granules and meltwater containing ^{210}Pb explains why the latter is always found at high concentrations in cryoconite, regardless of the geographic context. For artificial FRNs the case is different since they are not continuously deposited on the surface of glaciers; however, they are still present in cryoconite with high activities. Each year during the melting season part of the ice dating back to the peak of atmospheric nuclear tests and to major nuclear incidents melts out, releasing its artificial nuclide burden which is transported by meltwater. As for unsupported ^{210}Pb, cryoconite granules retain such nuclides owing to their biogeochemical properties and accumulate a load of artificial radioactivity even if decades have passed since its original deposition on glaciers. The ability of cryoconite is likely related to the presence of organic matter and extracellular polymeric substances which are affine for heavy metals, including the radioactive ones (Gadd, 1996; Fowler et al., 2010; Kim et al., 2011; Chuang et al., 2015). An additional support for the importance of organic matter in this process is also given by previous studies showing that the organic fraction of cryoconite and snow algae accumulates heavy metals associated with anthropogenic atmospheric emissions (Fjerdingstad, 1973; Nagatsuka et al., 2010; Łokas et al., 2016; Baccolo et al., 2017; Owens et al., 2019; Huang et al., 2019).

One observation might corroborate our hypothesis. Wilflinger et al. (2018) reported about high activity of ^{7}Be ($t_{1/2} = 53$ d) in their samples, up to 34 000 Bq kg^{-1}. ^{7}Be is a short-lived cosmogenic radionuclide, deposited from the atmosphere with precipitation. We observed ^{7}Be within our samples, but we could not properly quantify it because months passed between sampling and γ-spectrometry. Finding an excess of ^{7}Be in cryoconite, implies that, given its lifetime, the absorption by cryoconite granules took place in the weeks just before sampling and not when the cryoconite originally formed. The presence of short-lived nuclides suggests that cryoconite granules continuously accumulate radioactive species through the interaction not only with meltwater but also with rain, where ^{7}Be is always present.

According to our interpretation, cryoconite containing higher concentrations of radionuclides has formed on the glacier before cryoconite, presenting lower activities. Beyond this, however, we believe it is difficult to attempt a more precise dating through radioactive decay, even if it remains an interesting task. Too many processes are poorly understood to make a rigorous attempt at present; we first should understand the relationships which exist between the formation of cryoconite and of cryoconite granules, the geometry of the glacier, the age and displacement of ice, and in particular the exchanges between ice, meltwater and cryoconite granules.

5 Conclusions and future perspectives

We have described the ability of cryoconite to accumulate both artificial and natural FRNs. A comprehensive comparison against other environmental matrices revealed that cryoconite is, excluding samples from nuclear test and incident sites, one of the most radioactive natural substance found in Earth surface environments. Our study is focused on cryoconite samples from the European Alps, but results from other regions of the global cryosphere confirm our findings, proving that the accumulation of radioactivity is not a local phenomenon but involves worldwide glaciated areas. The accumulation of FRNs in cryoconite is so efficient that it has even allowed for a relatively easy detection of uncommon FRNs. Cryoconite is a promising tool in the fields of radioecology and environmental nuclear forensics.

The use of diagnostic ratios has shed light on the sources of radioactivity found in cryoconite. Results show that multiple sources, both regional and global, influence the radioactive signature of Alpine cryoconite. Pu-related nuclides reveal a dominant source of their presence to be the global stratospheric fallout from atmospheric nuclear tests carried out in the second half of the 20th century. In contrast, the major contribution for ^{137}Cs is determined to have come from the 1986 Chernobyl accident. The ability to record both planetary and more regional events is also suggested by a comparison with literature concerning other geographic contexts. Differences are observed and can be explained considering the impact of regional events. It is important to note that currently no information exists about the radioactivity of cryoconite from the Southern Hemisphere. Building a comprehensive picture of radioactivity in the global cryosphere is a geographic gap that it would be valuable to close.

There is evidence to suggest that the fundamental process which makes cryoconite a "sponge" for impurities in glacial environments, including radionuclides, is the interaction between ice and cryoconite itself, through the mediation of meltwater. When glaciers melt, they release and mobilize with meltwater the radionuclides originally preserved in snow and ice layers. Due to the organic matter content and its sticky properties, cryoconite efficiently binds and accumulates the impurities contained in meltwater, in particular those with an affinity for organic substances, including radionuclides.

This study has focused strictly on the glacial environment, ignoring the fate of cryoconite once it is released by glaciers and transported into the downstream ecosystems. It is likely that owing to meltwater discharge, the radioactivity accumulated in cryoconite is promptly diluted, avoiding any health

and ecotoxicological risk. However, caution should be taken considering those proglacial areas in close proximity to the ice, where the dilution could be limited, and some risks could exist. Given the global relevance of this phenomenon, further research should focus on the extra-glacial fate of cryoconite and the contaminants contained within it.

Data availability. All data are available in the Supplement.

Supplement. The supplement related to this article is available online at: https://doi.org/10.5194/tc-14-657-2020-supplement.

Author contributions. GB conceived the idea of this study, interpreted the data and wrote the manuscript with contributions from all the coauthors; RA, GB, BDM, AF and RSA collected the samples; GB, EŁ, PG and MN performed the radioactivity measurements and outlined the potential sources of radioactivity; DM and PP determined the carbonaceous content of cryoconite; GB, MN and MP carried out neutron activation analysis; CC, BD, VM and EP helped in the interpretation of the data; VM handled funding acquisition.

Competing interests. The authors declare that they have no conflict of interest.

Acknowledgements. We thank Herbert Lettner for sharing the data about cryoconite from Austrian glaciers. We also thank the two reviewers for the useful and constructive comments.

Financial support. This study has been supported by the Project of Strategic Interest NEXTDATA, funded by the Italian National Research Programme PNR 2011-2013, and by the MIAMI (Monitoraggio Inquinamento Atmosferico della Montagna Italiana) project, funded by "Dipartimento per gli affari regionali e le autonomie della Presidenza del Consiglio dei Ministri". Plutonium isotopic analyses have been supported by the Polish National Science Center (grant no. 2016/21/B/ST10/02327).

Review statement. This paper was edited by Ruth Mottram and reviewed by Elizabeth Bagshaw and one anonymous referee.

References

Aarkrog, A. and Dahlgaard, H.: Evidence for Bismuth-207 in Global Fallout, J. Environ. Radioactiv., 1, 107–117, 1984.

Abella, M. K. I. L., Rouco Molina, M., Nikolić-Hughes, I., Hughes, E. W., and Ruderman, M. A.: Background gamma radiation and soil activity measurements in the northern Marshall Islands, P. Natl. Acad. Sci. USA, 116, 15425–15434, https://doi.org/10.1073/pnas.1903421116, 2019.

Ambrosini, R., Azzoni, R. S., Pittino, F., Diolaiuti, G., and Franzetti, A., Parolini, M.: First evidence of microplastic contamination in the supraglacial debris of an alpine glacier, Environ. Pollut., 253, 297–301, 2019.

Appleby, P. G.: Three decades of dating recent sediments by fallout radionuclides: a review, Holocene, 18, 83–93, https://doi.org/10.1177/0959683607085598, 2008.

Avery, S. V.: Fate of caesium in the environment: Distribution between the abiotic and biotic components of aquatic and terrestrial ecosystems, J. Environ. Radioactiv., 30, 139–171, 1996.

Azzoni, R. S., Fugazza, D., Zennaro, M., Zucali, M., D'Agata, C., and Maragno, D.: Recent structural evolution of Forni glacier tongue (Ortles-Cevedale group, Central Italian Alps), J. Maps, 13, 870–878, 2017.

Baccolo, G., Di Mauro, B., Massabò, D., Clemenza, M., Nastasi, M., Delmonte, B., Prata, M., Prati, P., Previtali, E., and Maggi, V.: Cryoconite as a temporary sink for anthropogenic species stored in glaciers, Sci. Rep., 7, 9623, https://doi.org/10.1038/s41598-017-10220-5, 2017.

Bagshaw, E. A., Tranter, M., Fountain, A., G., Welch, K. A., Basagic, H., and Lyons, W. B.: Biogeochemical evolution of cryoconite holes in Canada glacier, Taylor Valley, Antarctica, J. Geophys. Res.-Biogeo., 112, G04S35, https://doi.org/10.1029/2007JG000442, 2007.

Bossew, P., Lettner, H., and Hubmer, A.: A note on ^{207}Bi in environmental samples, J. Environ. Radioactiv., 91, 160–166, 2006.

Bryan, S. E., McDonald, P., Hill, R., and Wilson, R. C.: Sea to land transfer of anthropogenic radionuclides to the North Wales coast, Part I: external gamma radiation and radionuclide concentrations in intertidal sediments, soil and air, J. Environ. Radioactiv., 99, 7–19, 2008.

Cagno, S., Hellemans, K., Lind, O. C., Skipperud, L., Janssens, K., and Salbu, B.: LA-ICP-MS for Pu source identification at Mayak PA, the Urals, Russia, Environ. Sci. Proc. Imp., 16, 306–312, 2014.

Chuang, C. Y., Santschi, P. H., Wen, L. S., Guo, L., Xu, C., Zhang, S., Jiang, Y., Schwer, K. A., Quigg, A., Hung, C. C., Ayranov, M., and Schumann, D.: Binding of Th, Pa, Pb, Po and Be radionuclides to marine colloidal macromolecular organic matter, Mar. Chem., 173, 320–329, 2015.

Cook, J., Edwards, A., Takeuchi, N., and Irvine-Fynn, T.: Cryoconite: the dark biological secret of the cryosphere, Prog. Phys. Geog., 40, 66–111, https://doi.org/10.1177/0309133315616574, 2015.

Cota, G. F., Cooper, L. W., Darby, D. A., and Larsen, I. L.: Unexpectedly high radioactivity burdens in ice-rafted sediments from the Canadian Arctic Archipelago, Sci. Total Environ., 366, 253–261, 2006.

Di Mauro, B., Baccolo, G., Garzonio, R., Giardino, C., Massabò, D., Piazzalunga, A., Rossini, M., and Colombo, R.: Impact of impurities and cryoconite on the optical properties of the Morteratsch Glacier (Swiss Alps), The Cryosphere, 11, 2393–2409, https://doi.org/10.5194/tc-11-2393-2017, 2017.

Diaconis, P., Goel, S., and Holmes, S.: Horseshoes in multidimensional scaling and local kernel methods, Ann. Appl. Stat., 2, 777–807, 2008.

Ferrario, C., Pittino, F., Tagliaferri, I., Gandolfi, I., Bestetti, G., Azzoni, R. S., Diolaiuti, G., Franzetti, A., Ambrosini, R., and Villa,

S.: Bacteria contribute to pesticide degradation in cryoconite holes in an Alpine glacier, Environ. Pollut., 230, 919–926, 2017.

Fjerdingstad, E.: Accumulated concentrations of heavy metals in red snow algae in Greenland, Schweiz. Z. Hydrol. 35, 247–251, 1973.

Fountain, A. G., Tranter, M., Nylen, T. H., Lewis, K. J., and Mueller, D. R.: Evolution of cryoconite holes and their contribution to meltwater runoff from glaciers in the McMurdo Dry Valleys, Antarctica, J. Glaciol., 50, 35–45, 2004.

Fowler, S. W.: ^{210}Po in the marine environment with emphasis on its behaviour within the biosphere, J. Environ. Radioactiv., 102, 448–461, 2011.

Fugazza, D., Senese, A., Azzoni, R. S., Maugeri, M., Maragno, D., and Diolaiuti, G. A.: New evidence of glacier darkening in the Ortles-Cevedale group from Landsat observations, Global Planet. Change, 178, 35–45, 2019.

Gadd, G. M.: Influence of microorganisms on the environmental fate of radionuclides, Endeavour, 20, 150–156, 1996.

Gückel, K., Shinonaga, T., Christl, M., and Tschiersch, J.: Scavenged ^{239}Pu, ^{240}Pu, and ^{241}Am from snowfalls in the atmosphere settling on Mt. Zugspitze in 2014, 2015 and 2016, Sci. Rep., 7, 11848, https://doi.org/10.1038/s41598-017-12079-y, 2017.

Guelle, W., Balkanski, Y. J., Dibb, J. E., Schulz, M., and Dulac, F.: Wet deposition in a global size-dependent aerosol transport model: 2. Influence of the scavenging scheme on ^{210}Pb vertical profiles, surface concentrations, and deposition, J. Geophys. Res.-Atmos., 103, 28875–28891, https://doi.org/10.1029/98JD01826, 1998.

Hirose, K., Igarashi, Y., and Aoyama, M.: Analysis of the 50-year records of the atmospheric deposition of long-lived radionuclides in Japan, Appl. Radiat. Isotopes, 66, 1675–1678, 2008.

Hodson, A. J.: Understanding the dynamics of black carbon and associated contaminants in glacial systems, Wiley Interdiscip. Rev. Waters, 1, 141–149, https://doi.org/10.1002/wat2.1016, 2014.

Hotaling, S., Bartholomaus, T. C., and Gilbert, S. L.: Rolling stones gather moss: movement and longevity of moss balls on an Alaskan glacier, Preprint at bioRxiv, available at: https://www.biorxiv.org/node/801466.full (last access: 12 February 2020), 2019.

Huang, J., Kang, S., Ma, M., Guo, J., Cong, Z., Dong, Z., Yin, R., Xu, J., Tripathee, L., Ram, K., and Wang, F.: Accumulation of atmospheric mercury in glacier cryoconite over Western China, Environ. Sci. Technol., 53, 6632–6639, 2019.

Jenk, T. M., Szidat, S., Schwikowski, M., Gäggeler, H. W., Brütsch, S., Wacker, L., Synal, H.-A., and Saurer, M.: Radiocarbon analysis in an Alpine ice core: record of anthropogenic and biogenic contributions to carbonaceous aerosols in the past (1650–1940), Atmos. Chem. Phys., 6, 5381–5390, https://doi.org/10.5194/acp-6-5381-2006, 2006.

Kaufmann, V., Plösch, R., Ritter, S., and Streber, J.: Documentation of the Glacier Retreat in the Eastern Part of the Granatspitz Mountains (Austrian Alps) Using Aerial Photographs for the Time Period 2003–2009, Cartogr. J., 50, 232–239, https://doi.org/10.1179/1743277413Y.0000000057, 2013.

Ketterer, M. E. and Szechenyi, S. C.: Determination of plutonium and other transuranic elements by inductively coupled plasma mass spectrometry: A historical perspective and new frontiers in the environmental sciences, Spectrochim. Acta B, 63, 719–737, 2008.

Kim, G., Hussain, N., Chureh, T. M., and Carey, W. L.: The fallout isotope ^{207}Bi in a Delaware salt marsh: a comparison with ^{210}Pb and ^{137}Cs as a geochronological tool, Sci. Total Environ., 196, 31–41, 1997.

Kim, G., Kim., T. H., and Church, T. M.: Po-210 in the environment: biogeochemical cycling and bioavailability, in: Handobbok of environmental isotope geochemistry, edited by: Baskaran, M., Springer, 271–284, 2011.

Kirchner, G. and Daillant, O.: The potential of lichens as long-term biomonitors of natural and artificial radionuclides, Environ. Pollut., 120, 145–150, 2002.

Langford, H., Hodson, A., Banwart, S., and Bøggild, C.: The microstructure and biogeochemistry of Arctic cryoconite granules, Ann. Glaciol., 51, 87–94, 2010.

Łokas, E., Zaborska, A., Kolicka, M., Różycki, M., and Zawierucha, K.: Accumulation of atmospheric radionuclides and heavy metals in cryoconite holes on an Arctic glacier, Chemosphere, 160, 162–172, 2016.

Łokas, E., Wachniew, P., Jodłowski, P., and Gasiorek, M.: Airborne radionuclides in the proglacial environment as indicators of sources and transfers of soil material, J. Environ. Radioactiv., 178–179, 193–202, 2017.

Łokas, E., Zawierucha, K., Cwanek, A., Szufa, K., Gaca, P., Mietelski, J. W., and Tomankiewicz, E.: The sources of high airborne radioactivity in cryoconite holes from the Caucasus (Georgia), Sci. Rep., 8, 10802, https://doi.org/10.1038/s41598-018-29076-4, 2018.

Łokas, E., Zaborska, A., Sobota, I., Gaca, P., Milton, J. A., Kocurek, P., and Cwanek, A.: Airborne radionuclides and heavy metals in high Arctic terrestrial environment as the indicators of sources and transfers of contamination, The Cryosphere, 13, 2075–2086, https://doi.org/10.5194/tc-13-2075-2019, 2019.

Lorenz, K., Preston, C. M., and Kandeler, E.: Soil organic matter in urban soils: Estimation of elemental carbon by thermal oxidation and characterization of organic matter by solid-state ^{13}C nuclear magnetic resonance (NMR) spectroscopy, Geoderma, 130, 312–323, 2006.

Meese, D. A., Reimnitz, E., Tucker III, W. B., Gow, A. J., Bischof, J., and Darby, D.: Evidence for radionuclide transport by sea ice, Sci. Total Environ., 202, 267–278, 1997.

Nagatzuka, N., Takeuchi, N., Nakano, T., Kokado, E., and Li., Z.: Sr, Nd and Pb stable isotopes of surface dust on Ürümki glacier No. 1 in western China, Ann. Glaciol., 51, 95–105, 2010.

Nifontova, M.: Radionuclides in the moss-lichen cover of tundra communities in the Yamal Peninsula, Sci. Total Environ., 160–161, 749–752, 1995.

Noshkin, V. E., Robison, W. L., Brunk, J. A., and Jokela, T. A.: An evaluation of activated bismuth isotopes in environmental samples from the former Western Pacific Proving Grounds, J. Radioanal. Nucl. Chem., 248, 741–750, 2001.

Osburn Jr., W. S.: The dynamics of fallout distribution in a Colorado alpine tundra snow accumulation ecosystem in: Radioecology, edited by: Schultz, V. and Klement, A. W., Reinhold Publishing Corporation, New York, 51–71, 1963.

Owens, P. N., Blake, W. H., and Millward, G. E.: Extreme levels of fallout radionuclides and other contaminants in glacial sediments (cryoconite) and implications for downstream acquatic ecosys-

tems, Sci. Rep., 9, : 12531, https://doi.org/10.1038/s41598-019-48873-z, 2019.

Pittino, F., Maglio, M., Gandolfi, I., Azzoni, R. S., Diolaiuti, G., Ambrosini, R., and Franzetti, A.: Bacterial communities of cryoconite holes of a temperate alpine glacier show both seasonal trends and year-to-year variability, Ann. Glaciol., 59, 1–9, 2018a.

Pittino, F., Ambrosini, R., Azzoni, R., Diolaiuti, G., Villa, S., Gandolfi, I., and Franzetti, A.: Post-depositional biodegradation processes of pollutants on glacier surfaces, Condens. Matter, 3, 24, https://doi.org/10.3390/condmat3030024, 2018b.

Pourcelot, L., Louvat, D., Gauthier-Lafaye, F., and Stille, P.: Formation of radioactivity enriched soils in mountain areas, J. Environ. Radioactiv., 68, 215–223, 2003.

Pribyl, D. W.: A critical review of the conventional SOC to SOM conversion factor, Geoderma, 156, 75–83, 2010.

Rudnick, R. L. and Gao S.: Composition of the continental crust, in: Treatise on Geochemistry, Vol. 3: the Crust, edited by: Rudnick, R. L., Elsevier, 1–64, 2003.

Sandalls, F. J., Segal, M. G., and Victorova, N.: Hot Particles from Chernobyl: A Review, J. Environ. Radioactiv., 18, 5–22, 1993.

Shabana, E. I. and Al-Shammari, H. L.: Assessment of the global fallout of plutonium isotopes and americium-241 in the soil of the central region of Saudi Arabia, J. Environ. Radioactiv., 57, 67–74, 2001.

Singh, S. M., Avinash, K., Sharma, P., Mulik, R. U., Upadhyay, A. K., and Ravindra, S.: Elemental variations in glacier cryoconites of Indian Himalaya and Spitsbergen, Arctic. Geosci. Front., 8, 1339–1347, 2017.

Steinhauser, G.: Environmental nuclear forensics: the need for a new scientific discipline, Environ. Sci. Pollut. Res., 26, 16901–16903, 2019.

Steinhauser, G., Merz, S., Hainz, D., and Sterba, J. H.: Artificial radioactivity in environmental media (air, rainwater, soil, vegetation) in Austria after the Fukushima nuclear accident, Environ. Sci. Pollut. R., 20, 2527–2534, 2013.

Steinhauser, G., Brandl, A., and Johnson, T. E.: Comparison of the Chernobyl and Fukushima nuclear accidents: A review of the environmental impacts, Sci. Total Environ., 470–471, 800–817, 2014.

Strawn, D. G. and Spark, D. L.: Effects of Soil Organic Matter on the Kinetics and Mechanisms of Pb(II) Sorption and Desorption in Soil, Soil Sci. Soc. Am. J., 64, 144–156, 2000.

Takeuchi, N., Kohshima, S., and Seko, K.: Structure, formation and darkening process of albedo-reducing material (Cryoconite) on a Himalayan glacier: a granular algal mat growing on the glacier, Arct. Antarc. Alp. Res., 33, 115–122, 2001.

Takeuchi, N., Sakaki, R., Uetake, J., Nagatsuka, N., Shimada, R., Niwano, M., and Aoki, T.: Temporal variations of cryoconite holes and cryoconite coverage on the ablation ice surface of Qaanaaq Glacier in northwest Greenland, Ann. Glaciol., 59, 21–30, https://doi.org/10.1017/aog.2018.19, 2018.

Thakur, P. and Ward, A. L.: ^{241}Pu in the environment: insight into the understudied isotope of plutonium, J. Radioanal. Nucl. Chem., 317, 757–778, 2018.

Tieber, A., Lettner, H., Bossew, P., Hubmer, A., Sattler, B., and Hofmann, W.: Accumulation of anthropogenic radionuclides in cryoconites on Alpine glaciers, J. Environ. Radioactiv., 100, 590–598, 2009.

Tomadin, L., Wagenbach, D., and Landuzzi, V.: Mineralogy and source of high altitude glacial deposits in the western Alps: clay minerals as Saharan dust tracers, in: The impact of desert dust across the Mediterranean, edited by: Guerzoni, S. and Chester, R., Kuwer Academic Publishers, 223–232, 1996.

van Dongen, S. and Enright, A. J.: Metric distances derived from cosine similarity and Pearson and Spearman correlations, Preprint at arXiv, available at: https://arxiv.org/abs/1208.3145 (last access: 12 February 2020), 2012.

Weiland-Bräuer, N., Fischer, M. A., Schramm, K. W., and Schmitz, R. A.: Polychlorinated Biphenyl (PCB)-Degrading Potential of Microbes Present in a Cryoconite of Jamtalferner Glacier, Front. Microbiol., 8, 105, https://doi.org/10.3389/fmicb.2017.01105, 2017.

Wilflinger, T., Lettner, H., Hubmer, A., Bossew, P., Sattler, B., and Slupetzky, H.: Cryoconites from Alpine glaciers: Radionuclide accumulation and age estimation with Pu and Cs isotopes and ^{210}Pb, J. Environ. Radioactiv., 186, 90–100, 2018.

Yasunari, T. J. Stohl, A., Hayano, R. S., Burkhart, J. F., Eckhardt, S., and Yasunari, T.: Cesium-137 deposition and contamination of Japanese soils due to the Fukushima nuclear accident, P. Natl. Acad. Sci. USA, 108, 19530–19534, https://doi.org/10.1073/pnas.1112058108, 2011.

Supplementary material to: "Cryoconite: an efficient accumulator of radioactive fallout in glacial environments"

Giovanni Baccolo[1,2], Edyta Łokas[3], Paweł Gaca[4], Dario Massabò[5,6], Roberto Ambrosini[7], Roberto S. Azzoni[7], Caroline Clason[8], Biagio Di Mauro[1], Andrea Franzetti[1], Massimiliano Nastasi[1,9], Michele Prata[10], Paolo Prati[5,6], Ezio Previtali[1,9], Barbara Delmonte[1], Valter Maggi[1,2]

1 Environmental and Earth Sciences Department, University of Milano-Bicocca, Milano, 20126, Italy.
2 INFN section of Milano-Bicocca, Milano, 20126, Italy.
3 Department of Nuclear Physical Chemistry, Institute of Nuclear Physics Polish Academy of Sciences, Kraków, 31-342, Poland.
4 Ocean and Earth Science, University of Southampton, National Oceanography Centre, Southampton, SO14 3ZH UK.
5 Physics Department, University of Genoa, Genoa, 16146, Italy.
6 INFN section of Genoa, Genoa, 16146, Italy.
7 Department of Environmental Science and Policy, University of Milan, Milano, 20133, Italy.
8 School of Geography, Earth and Environmental Sciences, University of Plymouth, Plymouth, PL48AA, UK.
9 Physics Department, University of Milano-Bicocca, Milano, 20126, Italy.
10 Laboratory of Applied Nuclear Energy, University of Pavia, Pavia, 27100, Italy.

Correspondence to: G. Baccolo (giovanni.baccolo@unimib.it)

In the following list the references whose data were used to create **Fig. 4**, are reported. Studies concerning sites where nuclear explosion tests and accidents occurred, were not taken into account. In addition to the listed studies, also the following references cited in the main text were used: Aarkrog and Dahlgaard, 1984; Kim et al., 1997, Kirchner et al., 2002.

- Aleksiayenak, Y. V., Frontasyeva, M. V., Florek, M., Sykora, I., Holy, K., Masarik, J., Brestakova, L., Jeskovsky, M., Steinnes, E., Faanhof, A., Ramatlhape, K. I.: Distributions of 137Cs and 210Pb in moss collected from Belarus and Slovakia. J. Environ. Radioactiv. 117, 19-24, 2013.
- Ali, A. A., Ghaleb, B., Garneau, M., Asnong, H., Loisel, J.: Recent peat accumulation rates in minerotrophic peatlands of the Bay James region, Eastern Canada, inferred by 210Pb and 137Cs radiometric techniques. Appl. Radiat. Isotopes 66, 1350-1358, 2008.
- Al Hamarneh, I., Wreikat, A., Toukan, K.: Radioactivity concentrations of 40K, 134Cs, 137Cs, 90Sr, 241Am, 238Pu and 239+ 240Pu radionuclides in Jordanian soil samples. J. Environ. Radioactiv. 67, 53-67, 2003.
- Baskaran, M., Asbill, S., Schwantes, J., Santschi, P., Champ, M. A., Brooks, J. M., Adkinson, D., Makeyev, V.: Concentrations of 137Cs, 239,240Pu and 210Pb in Sediment Samples from the Pechora Sea and Biological Samples from the Ob, Yenisey Rivers and Kara Sea. Mar. Pollut. Bull. 40, 830-838, 2000.

- Belivermiş, M. and Çotuk, Y.: Radioactivity measurements in moss (*Hypnum cupressiforme*) and lichen (*Cladonia rangiformis*) samples collected from Marmara region of Turkey. J. Environ. Radioactiv. 101, 945-951, 2010.
- Belivermiş, M., Kiliç, Ö., Çayir, A., Coşkun, M., Coşkun, M.: Assessment of 210Po and 210Pb in lichen, moss and soil around Çan coal-fired power plant, Turkey. J. Radional. Nucl. Chem. 307, 523-531, 2016.
- Breban, D. C., Moreno, J., Mocanu, N.: Activities of Pu radionuclides and 241Am in soil samples from an alpine pasture in Romania. J. Radional. Nucl. Chem. 258, 613-617, 2003.
- Caridi, F., Belvedere, A., D'Agostino, M., Marguccio, S.: 137Cs activity concentration in mosses in the Calabria region, south of Italy. J. Instrum. 12, DOI: 10.1088/1748-0221/12/05/P05001, 2017.
- Duffa, C., Renaud, P., Goutelard, F.: Activities and transfers of Pu and Am in rice samples from Camargue, France. J. Radioanal. Nucl. Chem. 252, 247-248, 2002.
- Ekdal, E., Karali, T., Saç, M. M.: 210Po and 210Pb in soils and vegetables in Kucuk Menderes basin of Turkey. Radiat. Meas. 41, 72-77, 2006.
- Figueira, R. C. L., Tessler, M. G., de Mahiques, M. M., Cunha, I. I. L.: Distribution of 137Cs, 238Pu and 239 + 240Pu in sediments of the southeastern Brazilian shelf–SW Atlantic margin. Sci. Total Environ. 357, 146-159, 2006.
- Gascò, C., Antón, M. P., Pozuelo, M., Meral, J., Gonzáles, A. M., Papucci, C., Delfanti, R.: Distributions of Pu, Am and Cs in margin sediments from the western Mediterranean (Spanish coast). J. Environ. Radioactiv. 59, 75-89, 2002.
- He, Q. and Dwelling, D. E.: The distribution of fallout 137Cs and 210Pb in undisturbed and cultivated soil. Appl. Radiat. Isotopes 48, 677-690, 1997.
- Heldal, H. E., Varskog, P., Føyn, L.: Distribution of selected anthropogenic radionuclides (137Cs, 238Pu, 239,240Pu and 241Am) in marine sediments with emphasis on the Spitsbergen–Bear Island area. Sci. Total Environ. 293, 233-245, 2002.
- Huh, C. A. and Su, C. C.: Distribution of fallout radionuclides (7Be, 137Cs, 210Pb and 239,240Pu) in soils of Taiwan. J. Environ. Radioactiv. 77, 78-100, 2004.
- Ishikawa, Y., Sato, N., Yoshihara, K.: 207Bi and other fallout nuclides in sea sediments in relation to ignition loss of samples. J. Radioanal. Nucl. Chem. 137, 67-74, 1989.
- Jenkins, C. E., Wogman, N. A., Rieck, H. G.: Radionuclide distribution in olympic national park, Washington. Water Air Soil Poll. 1, 181-204, 1972.

- Jia, G., Triulzi, C., Nonnis Marzano, F., Belli, M., Vaghi, M.: The fate of plutonium, 241Am, 90Sr and 137Cs in the Antarctic ecosystem. Antarctic Science 12, 141-148, 2000.
- Joshi, S. and McNeely, R.: Detection of fallout 155Eu and 207Bi in a 210Pb-dated lake sediment core. J. Radioanal. Nucl. Chem. 122, 183-191, 1988.
- Kahraman, A., Kaynak, G., Akkaya, G., Gürler, O., Yalçın, S.: Radioactivity measurements in epiphytic lichens of Uludağ Mountain in Western Anatolia. J. Radional. Nucl. Chem. 295, 1057-1066, 2013.
- Ketterer, M. E., Hafer, K. M., Mietelski, J. W.: Resolving Chernobyl vs. global fallout contributions in soils from Poland using Plutonium atom ratios measured by inductively coupled plasma mass spectrometry. J. Environ. Radioactiv. 73, 183-201, 2004.
- Komura, K.: Bismuth-207 in environmental samples. Radioisotopes 34, 555-558, 1985.
- Krmar, M., Wattanavatee, K., Radnović, D., Slivka, J., Bhongsuwan, T., Frontasyeva, M. V., Pavlov, S. S.: Airborne radionuclides in mosses collected at different latitudes. J. Environ. Radioactiv. 117, 45-48, 2013.
- LaBrecque, J. J. and Cordoves, P. R.: Determination and spatial distribution of 137Cs in soils, mosses and lichens near Kavanayen, Venezuela. J. Radional. Nucl. Chem. 273, 401-404, 2007.
- Lee, M. H. and Lee, C. W.: Association of fallout -derived 137Cs, 90Sr and 239,240Pu with natural organic substances in soils. J. Environ. Radioactiv. 47, 253-262, 2000.
- Lee, M. H., Lee, C. W., Boo, B. H.: Distribution and characteristics of 239,240Pu and 137Cs in the soil of Korea. J. Environ. Radioactiv. 37, 1-16, 1997.
- Lee, S. H., Povinec, P. P., Wyse, E., Pham, M. K., Hong, G. H., Chung, C. S., Kim, S. H., Lee, H. J.: Distribution and inventories of 90Sr, 137Cs, 241Am and Pu isotopes in sediments of the Northwest Pacific Ocean. Mar. Geol. 216, 249-263, 2005.
- Lee, S. H., Oh, J. S., Lee, J. M., Lee, K. B., Park, T. S., Lujaniene, G., Valiulis, D., Šakalis, J.: Distribution characteristics of 137Cs, Pu isotopes and 241Am in soil in Korea. Appl. Radiat. Isotopes 81, 315-320, 2013.
- Li, C. X., Le Roux, G., Sonke, J., van Beek, P., Souhaut, M., Van der Putten, N., De Vleeschouwer, F.: Recent 210Pb, 137Cs and 241Am accumulation in an ombrotrophic peatland from Amsterdam Island (Southern Indian Ocean). J. Environ. Radioactiv. 175-176, 164-169, 2017.
- Lindhal, P., Roos, P., Eriksson, M., Holm, E.: Distribution of Np and Pu in Swedish lichen samples (Cladonia stellaris) contaminated by atmospheric fallout. J. Environ. Radioactiv. 73, 73-85, 2004.
- Łokas, E., Mietelski, J. W., Ketterer, M. E., Klesczc, K., Wachniew, P., Michalska, S., Miecznik, M.: Sources and vertical distribution of 137Cs, 238Pu, 239+240Pu and 241Am in peat profiles from southwest Spitsbergen. Appl. Radiati. Isotopes 28, 100-108, 2013.

- Łokas, E., Bartmiński, P., Wachniew, P., Mietelski, J. W., Kawiak, T., Środoń, J.: Sources and pathways of artificial radionuclides to soils at a High Arctic site. Environ. Sci. Pollut. R. 21, 12479-12493, 2014.
- Machart, P., Hoffman, W., Türk, R., Steger,F.: Ecological half-life of 137Cs in lichens in an alpine region. J. Environ. Radioactiv. 97, 70-75, 2007.
- Mietelski, J. W., Olech, M. A., Sobiech-Matura, K., Howard, B. J., Gaca, P., Zwolak, M., Błażej, S., Tomankiewicz, E.: 137Cs, 40K, 238Pu, 239+240Pu and 90Sr in biological samples from King George Island (Southern Shetlands) in Antarctica. J. Environ. Radioactiv. 31, 1081-1089, 2008.
- Mietelski, J. W., Gaca, P., Olech, M.: Radioactive contamination of lichens and mosses collected in South Shetlands and Antarctic Peninsula. J. Radional. Nucl. Chem. 245, 527-537, 2000.
- Mietelski, J. W., Kubica, B., Gaca, P., Tomankievicz, E., Błażej, S., Tuteja-Krysa, M., Stobiński, M.: 238Pu, 239+240Pu, 241Am, 90Sr and 137Cs in mountain soil samples from the Tatra National Park (Poland). J. Radioanal. Nucl. Chem. 275, 523-533, 2008.
- Mróz, T., Łokas, E., Kocurek, J., Gąsiorek, M.: Atmospheric fallout radionuclides in peatland from Southern Poland. J. Environ. Radioactiv. 175-176, 25-33, 2017.
- Navas, A., Soto, J., Machìn, J.: 238U, 226Ra, 210Pb, 232Th and 40K activities in soil profiles of the Flysch sector (central Spanish Pyrenees). Appl. Radiat. Isotopes 57, 579-589, 2002.
- Outula, I.: Effect of industrial pollution on the distribution of Pu and Am in soil and on soil-to-plant transfer of Pu and Am in a pine forest in SW Finland. J. Radioanal. Nucl. Chem. 257, 267-274, 2003.
- Popov, L., Mihailova, G., Naidenov, I.: Detemination of activity ratios of 238,239,240Pu, 241Am, 134,137Cs, and 90Sr in Bulgarian soils. J. Radioanal. Nucl. Chem. 285, 223-237, 2010.
- Quank, N. H., Long, N. Q., Lieu, D. B., Mai, T. T., Ha, N. T., Nhan, D. D., Hien, P. D.: 239+240Pu, 90Sr and 137Cs inventories in surface soils of Vietnam. J. Environ. Radioactiv. 75, 329-337, 2004.
- Rezzoug, S., Michel, H., Fernex, F., Barci-Funel, G., Barci, V.: Evaluation of 137Cs fallout from the Chernobyl accident in a forest soil and its impact on Alpine Lake sediments, Mercantour Massif, S.E. France. J. Environ. Radioactiv. 85, 369-379, 2006.
- Schertz, M., Michel, H., Barci-Funel, G., Barci, V.: Transuranic and fission product contamination in lake sediments from an alpine wetland, Boréon (France). J. Environ. Radioactiv. 85, 380-388, 2006.
- Schuller, P., Voigt, G., Handl, J., Ellies, A., Oliva, L.: Global weapons' fallout 137Cs in soils and transfer to vegetation in south–central Chile. J. Environ. Radioactiv. 62, 181-193, 2002.
- Shabana, E. I. and Al-Shammari, H. L.: Assessment of the global fallout of plutonium isotopes and americium-241 in the soil of the central region of Saudi Arabia. J. Environ. Radioactiv. 57, 67-74, 2001.

- Skuterud, L., Gwynn, J. P., Gaare, E., Steinnes, E., Hove, K.: 90Sr, 210Po and 210Pb in lichen and reindeer in Norway. J. Environ. Radioactiv. 84, 441-456, 2005.
- Testa, C., Jia, G., Degetto, S., Desideri, D., Guerra, F., Meli, M. A., Rosselli, C.: Vertical profiles of 239,240Pu and 241Am in two sphagnum mosses of Italian peat. Sci. Total Environ. 232, 27-31, 1999.
- Uğur, A., Özden, B., Saç, M. M., Yener, G.: Biomonitoring of 210Po and 210Pb using lichens and mosses around a uraniferous coal-fired power plant in western Turkey. Atmos. Environ. 37, 2237-2245, 2003.
- Wattanawatee, K., Krmar, M., Bhogsuwan, T.: A survey of natural terrestrial and airborne radionuclides in moss samples from the peninsular Thailand. J. Environ. Radioactiv. 177, 113-127, 2017.

	Morteratsch	Forni
^{137}Cs (Bq kg^{-1})	2,650 ± 3,800	2,000 ±2,800
^{207}Bi (Bq kg^{-1})	9.4 ± 6.6	5.7 ± 2.4
^{238}Pu (Bq kg^{-1})	2.6 ± 2.5	0.22 ± 0.08
^{239,240}Pu (Bq kg^{-1})	78 ± 77	4.9 ± 0.9
^{241}Am (Bq kg^{-1})	30 ± 36	4.4 ± 1.6
^{40}K (Bq kg^{-1})	810 ± 55	750 ± 200
^{238}U (Bq kg^{-1})	68 ± 14	61 ± 22
^{234}Th (Bq kg^{-1})	88 ± 15	65 ± 17
^{214}Pb (Bq kg^{-1})	57 ± 7	44 ± 11
^{214}Bi (Bq kg^{-1})	57 ± 8	45 ± 12
Supp. ^{210}Pb (Bq kg^{-1})	69 ± 6	55 ± 17
Unsupp. ^{210}Pb (Bq kg^{-1})	2,700 ± 750	6,100 ± 1,850
^{232}Th (Bq kg^{-1})	65 ± 9	72 ± 6
^{228}Ac (Bq kg^{-1})	47 ± 5	53 ± 12
^{224}Ra (Bq kg^{-1})	34 ± 12	38 ± 17
^{212}Pb (Bq kg^{-1})	50 ± 3	54 ± 12
^{212}Bi (Bq kg^{-1})	52 ± 7	60 ± 15
^{208}Tl (Bq kg^{-1})	49 ± 5	50 ± 12
Organic Carbon (m/m %)	4.7 ± 0.8	3.6 ± 0.5
Elemental Carbon (m/m %)	0.49 ± 0.25	0.21 ± 0.12

Tab. S1 Average composition of cryoconite from the Morteratsch and Forni glaciers. Average data (± standard deviations) concerning the activity concentration of radionuclides and of carbonaceous matter are reported with respect to the two glaciers considered in this study.

Decay Chain	Radionucl.	$T_{1/2}$	γ-line energy (keV)	Eff. · B.R. (%)	Minimum Detectable Activity (Bq kg^{-1})	Average Uncertainty (%)
^{238}U – natural	^{210}Pb	22.3 yr	46.5	2.8	17.3	5.9
none – artificial	^{241}Am	432.2 yr	59.5	28.2	1.7	13
^{238}U – natural	^{234}Th	24.1 d	92.3-92.8	2.8	17.7	13
^{232}Th – natural	^{212}Pb	10.64 hr	238.6	24.6	1.9	7.8
^{232}Th – natural	^{224}Ra	3.66	241.0*	25.8	21.1	35
^{238}U – natural	^{214}Pb	26.8 min	295.2	9.5	4.7	12
^{232}Th – natural	^{228}Ac	6.15 hr	338.3	4.2	11.5	17
^{238}U – natural	^{214}Pb	26.8 min	351.9	15.0	3.1	9.1
^{232}Th – natural	^{208}Tl	3.05 min	583.2	3.2	7.4	16
^{238}U – natural	^{214}Bi	19.9 min	609.3	5.2	4.6	13
none – artificial	^{137}Cs	30.07 yr	661.7	20.4	0.7	5.5
^{232}Th – natural	^{212}Bi	60.55 min	727.3	1.1	11.2	27
^{232}Th – natural	^{208}Tl	3.05 min	860.6	0.6	17.1	39
^{232}Th – natural	^{228}Ac	6.15 hr	911.2	3.7	2.9	13
none – artificial	^{207}Bi	31.55 yr	1063.7	4.5	2.6	32
none – natural	^{40}K	$1.3 \cdot 10^9$ yr	1460.8	1.3	6.6	7.4
^{238}U – natural	^{214}Bi	19.9 min	1764.5	1.6	4.4	15
^{232}Th – natural	^{208}Tl	3.05 min	2614.5	0.7	7.9	28

Tab. S2 Details about γ-spectrometry. For each of the analysed nuclides the relevant analytical information is reported. B.R. corresponds to branching ratio. For the emission at 241 keV from ^{224}Ra (marked by an asterisk), a correction was needed to remove an interfering contribution from ^{214}Pb.

Supplement of The Cryosphere, 14, 657–672, 2020
https://doi.org/10.5194/tc-14-657-2020-supplement

The Cryosphere Open Access EGU

Supplement of

Cryoconite: an efficient accumulator of radioactive fallout in glacial environments

Giovanni Baccolo et al.

Correspondence to: Giovanni Baccolo (giovanni.baccolo@unimib.it)

- tc-14-657-2020-supplement-title-page.pdf
- Supplementary
  - S1_DataFile.xlsx
  - Supplementary material Cryosphere_Revised.pdf

Supplementary material to: "Cryoconite: an efficient accumulator of radioactive fallout in glacial environments"

Giovanni Baccolo[1,2], Edyta Łokas[3], Paweł Gaca[4], Dario Massabò[5,6], Roberto Ambrosini[7], Roberto S. Azzoni[7], Caroline Clason[8], Biagio Di Mauro[1], Andrea Franzetti[1], Massimiliano Nastasi[1,9], Michele Prata[10], Paolo Prati[5,6], Ezio Previtali[1,9], Barbara Delmonte[1], Valter Maggi[1,2]

[1] Environmental and Earth Sciences Department, University of Milano-Bicocca, Milano, 20126, Italy.
[2] INFN section of Milano-Bicocca, Milano, 20126, Italy.
[3] Department of Nuclear Physical Chemistry, Institute of Nuclear Physics Polish Academy of Sciences, Kraków, 31-342, Poland.
[4] Ocean and Earth Science, University of Southampton, National Oceanography Centre, Southampton, SO14 3ZH UK.
[5] Physics Department, University of Genoa, Genoa, 16146, Italy.
[6] INFN section of Genoa, Genoa, 16146, Italy.
[7] Department of Environmental Science and Policy, University of Milan, Milano, 20133, Italy.
[8] School of Geography, Earth and Environmental Sciences, University of Plymouth, Plymouth, PL48AA, UK.
[9] Physics Department, University of Milano-Bicocca, Milano, 20126, Italy.
[10] Laboratory of Applied Nuclear Energy, University of Pavia, Pavia, 27100, Italy.

Correspondence to: G. Baccolo (giovanni.baccolo@unimib.it)

In the following list the references whose data were used to create **Fig. 4**, are reported. Studies concerning sites where nuclear explosion tests and accidents occurred, were not taken into account. In addition to the listed studies, also the following references cited in the main text were used: Aarkrog and Dahlgaard, 1984; Kim et al., 1997, Kirchner et al., 2002.

- Aleksiayenak, Y. V., Frontasyeva, M. V., Florek, M., Sykora, I., Holy, K., Masarik, J., Brestakova, L., Jeskovsky, M., Steinnes, E., Faanhof, A., Ramatlhape, K. I.: Distributions of 137Cs and 210Pb in moss collected from Belarus and Slovakia. J. Environ. Radioactiv. 117, 19-24, 2013.
- Ali, A. A., Ghaleb, B., Garneau, M., Asnong, H., Loisel, J.: Recent peat accumulation rates in minerotrophic peatlands of the Bay James region, Eastern Canada, inferred by 210Pb and 137Cs radiometric techniques. Appl. Radiat. Isotopes 66, 1350-1358, 2008.
- Al Hamarneh, I., Wreikat, A., Toukan, K.: Radioactivity concentrations of 40K, 134Cs, 137Cs, 90Sr, 241Am, 238Pu and 239+ 240Pu radionuclides in Jordanian soil samples. J. Environ. Radioactiv. 67, 53-67, 2003.
- Baskaran, M., Asbill, S., Schwantes, J., Santschi, P., Champ, M. A., Brooks, J. M., Adkinson, D., Makeyev, V.: Concentrations of 137Cs, 239,240Pu and 210Pb in Sediment Samples from the Pechora Sea and Biological Samples from the Ob, Yenisey Rivers and Kara Sea. Mar. Pollut. Bull. 40, 830-838, 2000.

- Belivermiş, M. and Çotuk, Y.: Radioactivity measurements in moss (*Hypnum cupressiforme*) and lichen (*Cladonia rangiformis*) samples collected from Marmara region of Turkey. J. Environ. Radioactiv. 101, 945-951, 2010.
- Belivermiş, M., Kiliç, Ö., Çayir, A., Coşkun, M., Coşkun, M.: Assessment of 210Po and 210Pb in lichen, moss and soil around Çan coal-fired power plant, Turkey. J. Radional. Nucl. Chem. 307, 523-531, 2016.
- Breban, D. C., Moreno, J., Mocanu, N.: Activities of Pu radionuclides and 241Am in soil samples from an alpine pasture in Romania. J. Radional. Nucl. Chem. 258, 613-617, 2003.
- Caridi, F., Belvedere, A., D'Agostino, M., Marguccio, S.: 137Cs activity concentration in mosses in the Calabria region, south of Italy. J. Instrum. 12, DOI: 10.1088/1748-0221/12/05/P05001, 2017.
- Duffa, C., Renaud, P., Goutelard, F.: Activities and transfers of Pu and Am in rice samples from Camargue, France. J. Radioanal. Nucl. Chem. 252, 247-248, 2002.
- Ekdal, E., Karali, T., Saç, M. M.: 210Po and 210Pb in soils and vegetables in Kucuk Menderes basin of Turkey. Radiat. Meas. 41, 72-77, 2006.
- Figueira, R. C. L., Tessler, M. G., de Mahiques, M. M., Cunha, I. I. L.: Distribution of 137Cs, 238Pu and 239 + 240Pu in sediments of the southeastern Brazilian shelf–SW Atlantic margin. Sci. Total Environ. 357, 146-159, 2006.
- Gascò, C., Antón, M. P., Pozuelo, M., Meral, J., Gonzáles, A. M., Papucci, C., Delfanti, R.: Distributions of Pu, Am and Cs in margin sediments from the western Mediterranean (Spanish coast). J. Environ. Radioactiv. 59, 75-89, 2002.
- He, Q. and Dwelling, D. E.: The distribution of fallout 137Cs and 210Pb in undisturbed and cultivated soil. Appl. Radiat. Isotopes 48, 677-690, 1997.
- Heldal, H. E., Varskog, P., Føyn, L.: Distribution of selected anthropogenic radionuclides (137Cs, 238Pu, 239,240Pu and 241Am) in marine sediments with emphasis on the Spitsbergen–Bear Island area. Sci. Total Environ. 293, 233-245, 2002.
- Huh, C. A. and Su, C. C.: Distribution of fallout radionuclides (7Be, 137Cs, 210Pb and 239,240Pu) in soils of Taiwan. J. Environ. Radioactiv. 77, 78-100, 2004.
- Ishikawa, Y., Sato, N., Yoshihara, K.: 207Bi and other fallout nuclides in sea sediments in relation to ignition loss of samples. J. Radioanal. Nucl. Chem. 137, 67-74, 1989.
- Jenkins, C. E., Wogman, N. A., Rieck, H. G.: Radionuclide distribution in olympic national park, Washington. Water Air Soil Poll. 1, 181-204, 1972.

- Jia, G., Triulzi, C., Nonnis Marzano, F., Belli, M., Vaghi, M.: The fate of plutonium, 241Am, 90Sr and 137Cs in the Antarctic ecosystem. Antarctic Science 12, 141-148, 2000.
- Joshi, S. and McNeely, R.: Detection of fallout 155Eu and 207Bi in a 210Pb-dated lake sediment core. J. Radioanal. Nucl. Chem. 122, 183-191, 1988.
- Kahraman, A., Kaynak, G., Akkaya, G., Gürler, O., Yalçın, S.: Radioactivity measurements in epiphytic lichens of Uludağ Mountain in Western Anatolia. J. Radional. Nucl. Chem. 295, 1057-1066, 2013.
- Ketterer, M. E., Hafer, K. M., Mietelski, J. W.: Resolving Chernobyl vs. global fallout contributions in soils from Poland using Plutonium atom ratios measured by inductively coupled plasma mass spectrometry. J. Environ. Radioactiv. 73, 183-201, 2004.
- Komura, K.: Bismuth-207 in environmental samples. Radioisotopes 34, 555-558, 1985.
- Krmar, M., Wattanavatee, K., Radnović, D., Slivka, J., Bhongsuwan, T., Frontasyeva, M. V., Pavlov, S. S.: Airborne radionuclides in mosses collected at different latitudes. J. Environ. Radioactiv. 117, 45-48, 2013.
- LaBrecque, J. J. and Cordoves, P. R.: Determination and spatial distribution of 137Cs in soils, mosses and lichens near Kavanayen, Venezuela. J. Radional. Nucl. Chem. 273, 401-404, 2007.
- Lee, M. H. and Lee, C. W.: Association of fallout -derived 137Cs, 90Sr and 239,240Pu with natural organic substances in soils. J. Environ. Radioactiv. 47, 253-262, 2000.
- Lee, M. H., Lee, C. W., Boo, B. H.: Distribution and characteristics of 239,240Pu and 137Cs in the soil of Korea. J. Environ. Radioactiv. 37, 1-16, 1997.
- Lee, S. H., Povinec, P. P., Wyse, E., Pham, M. K., Hong, G. H., Chung, C. S., Kim, S. H., Lee, H. J.: Distribution and inventories of 90Sr, 137Cs, 241Am and Pu isotopes in sediments of the Northwest Pacific Ocean. Mar. Geol. 216, 249-263, 2005.
- Lee, S. H., Oh, J. S., Lee, J. M., Lee, K. B., Park, T. S., Lujaniene, G., Valiulis, D., Śakalis, J.: Distribution characteristics of 137Cs, Pu isotopes and 241Am in soil in Korea. Appl. Radiat. Isotopes 81, 315-320, 2013.
- Li, C. X., Le Roux, G., Sonke, J., van Beek, P., Souhaut, M., Van der Putten, N., De Vleeschouwer, F.: Recent 210Pb, 137Cs and 241Am accumulation in an ombrotrophic peatland from Amsterdam Island (Southern Indian Ocean). J. Environ. Radioactiv. 175-176, 164-169, 2017.
- Lindhal, P., Roos, P., Eriksson, M., Holm, E.: Distribution of Np and Pu in Swedish lichen samples (Cladonia stellaris) contaminated by atmospheric fallout. J. Environ. Radioactiv. 73, 73-85, 2004.
- Łokas, E., Mietelski, J. W., Ketterer, M. E., Klesczc, K., Wachniew, P., Michalska, S., Miecznik, M.: Sources and vertical distribution of 137Cs, 238Pu, 239+240Pu and 241Am in peat profiles from southwest Spitsbergen. Appl. Radiati. Isotopes 28, 100-108, 2013.

- Łokas, E., Bartmiński, P., Wachniew, P., Mietelski, J. W., Kawiak, T., Środoń, J.: Sources and pathways of artificial radionuclides to soils at a High Arctic site. Environ. Sci. Pollut. R. 21, 12479-12493, 2014.
- Machart, P., Hoffman, W., Türk, R., Steger,F.: Ecological half-life of 137Cs in lichens in an alpine region. J. Environ. Radioactiv. 97, 70-75, 2007.
- Mietelski, J. W., Olech, M. A., Sobiech-Matura, K., Howard, B. J., Gaca, P., Zwolak, M., Błażej, S., Tomankiewicz, E.: 137Cs, 40K, 238Pu, 239+240Pu and 90Sr in biological samples from King George Island (Southern Shetlands) in Antarctica. J. Environ. Radioactiv. 31, 1081-1089, 2008.
- Mietelski, J. W., Gaca, P., Olech, M.: Radioactive contamination of lichens and mosses collected in South Shetlands and Antarctic Peninsula. J. Radional. Nucl. Chem. 245, 527-537, 2000.
- Mietelski, J. W., Kubica, B., Gaca, P., Tomankievicz, E., Błaźej, S., Tuteja-Krysa, M., Stobiński, M.: 238Pu, 239+240Pu, 241Am, 90Sr and 137Cs in mountain soil samples from the Tatra National Park (Poland). J. Radioanal. Nucl. Chem. 275, 523-533, 2008.
- Mróz, T., Łokas, E., Kocurek, J., Gąsiorek, M.: Atmospheric fallout radionuclides in peatland from Southern Poland. J. Environ. Radioactiv. 175-176, 25-33, 2017.
- Navas, A., Soto, J., Machìn, J.: 238U, 226Ra, 210Pb, 232Th and 40K activities in soil profiles of the Flysch sector (central Spanish Pyrenees). Appl. Radiat. Isotopes 57, 579-589, 2002.
- Outula, I.: Effect of industrial pollution on the distribution of Pu and Am in soil and on soil-to-plant transfer of Pu and Am in a pine forest in SW Finland. J. Radioanal. Nucl. Chem. 257, 267-274, 2003.
- Popov, L., Mihailova, G., Naidenov, I.: Detemination of activity ratios of 238,239,240Pu, 241Am, 134,137Cs, and 90Sr in Bulgarian soils. J. Radioanal. Nucl. Chem. 285, 223-237, 2010.
- Quank, N. H., Long, N. Q., Lieu, D. B., Mai, T. T., Ha, N. T., Nhan, D. D., Hien, P. D.: 239+240Pu, 90Sr and 137Cs inventories in surface soils of Vietnam. J. Environ. Radioactiv. 75, 329-337, 2004.
- Rezzoug, S., Michel, H., Fernex, F., Barci-Funel, G., Barci, V.: Evaluation of 137Cs fallout from the Chernobyl accident in a forest soil and its impact on Alpine Lake sediments, Mercantour Massif, S.E. France. J. Environ. Radioactiv. 85, 369-379, 2006.
- Schertz, M., Michel, H., Barci-Funel, G., Barci, V.: Transuranic and fission product contamination in lake sediments from an alpine wetland, Boréon (France). J. Environ. Radioactiv. 85, 380-388, 2006.
- Schuller, P., Voigt, G., Handl, J., Ellies, A., Oliva, L.: Global weapons' fallout 137Cs in soils and transfer to vegetation in south–central Chile. J. Environ. Radioactiv. 62, 181-193, 2002.
- Shabana, E. I. and Al-Shammari, H. L.: Assessment of the global fallout of plutonium isotopes and americium-241 in the soil of the central region of Saudi Arabia. J. Environ. Radioactiv. 57, 67-74, 2001.

- Skuterud, L., Gwynn, J. P., Gaare, E., Steinnes, E., Hove, K.: 90Sr, 210Po and 210Pb in lichen and reindeer in Norway. J. Environ. Radioactiv. 84, 441-456, 2005.
- Testa, C., Jia, G., Degetto, S., Desideri, D., Guerra, F., Meli, M. A., Rosselli, C.: Vertical profiles of 239,240Pu and 241Am in two sphagnum mosses of Italian peat. Sci. Total Environ. 232, 27-31, 1999.
- Uğur, A., Özden, B., Saç, M. M., Yener, G.: Biomonitoring of 210Po and 210Pb using lichens and mosses around a uraniferous coal-fired power plant in western Turkey. Atmos. Environ. 37, 2237-2245, 2003.
- Wattanawatee, K., Krmar, M., Bhogsuwan, T.: A survey of natural terrestrial and airborne radionuclides in moss samples from the peninsular Thailand. J. Environ. Radioactiv. 177, 113-127, 2017.

	Morteratsch	Forni
^{137}Cs (Bq kg^{-1})	2,650 ± 3,800	2,000 ±2,800
^{207}Bi (Bq kg^{-1})	9.4 ± 6.6	5.7 ± 2.4
^{238}Pu (Bq kg^{-1})	2.6 ± 2.5	0.22 ± 0.08
^{239,240}Pu (Bq kg^{-1})	78 ± 77	4.9 ± 0.9
^{241}Am (Bq kg^{-1})	30 ± 36	4.4 ± 1.6
^{40}K (Bq kg^{-1})	810 ± 55	750 ± 200
^{238}U (Bq kg^{-1})	68 ± 14	61 ± 22
^{234}Th (Bq kg^{-1})	88 ± 15	65 ± 17
^{214}Pb (Bq kg^{-1})	57 ± 7	44 ± 11
^{214}Bi (Bq kg^{-1})	57 ± 8	45 ± 12
Supp. ^{210}Pb (Bq kg^{-1})	69 ± 6	55 ± 17
Unsupp. ^{210}Pb (Bq kg^{-1})	2,700 ± 750	6,100 ± 1,850
^{232}Th (Bq kg^{-1})	65 ± 9	72 ± 6
^{228}Ac (Bq kg^{-1})	47 ± 5	53 ± 12
^{224}Ra (Bq kg^{-1})	34 ± 12	38 ± 17
^{212}Pb (Bq kg^{-1})	50 ± 3	54 ± 12
^{212}Bi (Bq kg^{-1})	52 ± 7	60 ± 15
^{208}Tl (Bq kg^{-1})	49 ± 5	50 ± 12
Organic Carbon (m/m %)	4.7 ± 0.8	3.6 ± 0.5
Elemental Carbon (m/m %)	0.49 ± 0.25	0.21 ± 0.12

Tab. S1 Average composition of cryoconite from the Morteratsch and Forni glaciers. Average data (± standard deviations) concerning the activity concentration of radionuclides and of carbonaceous matter are reported with respect to the two glaciers considered in this study.

Decay Chain	Radionucl.	$T_{1/2}$	γ-line energy (keV)	Eff. · B.R. (%)	Minimum Detectable Activity (Bq kg^{-1})	Average Uncertainty (%)
^{238}U – natural	^{210}Pb	22.3 yr	46.5	2.8	17.3	5.9
none – artificial	^{241}Am	432.2 yr	59.5	28.2	1.7	13
^{238}U – natural	^{234}Th	24.1 d	92.3-92.8	2.8	17.7	13
^{232}Th – natural	^{212}Pb	10.64 hr	238.6	24.6	1.9	7.8
^{232}Th – natural	^{224}Ra	3.66	241.0*	25.8	21.1	35
^{238}U – natural	^{214}Pb	26.8 min	295.2	9.5	4.7	12
^{232}Th – natural	^{228}Ac	6.15 hr	338.3	4.2	11.5	17
^{238}U – natural	^{214}Pb	26.8 min	351.9	15.0	3.1	9.1
^{232}Th – natural	^{208}Tl	3.05 min	583.2	3.2	7.4	16
^{238}U – natural	^{214}Bi	19.9 min	609.3	5.2	4.6	13
none – artificial	^{137}Cs	30.07 yr	661.7	20.4	0.7	5.5
^{232}Th – natural	^{212}Bi	60.55 min	727.3	1.1	11.2	27
^{232}Th – natural	^{208}Tl	3.05 min	860.6	0.6	17.1	39
^{232}Th – natural	^{228}Ac	6.15 hr	911.2	3.7	2.9	13
none – artificial	^{207}Bi	31.55 yr	1063.7	4.5	2.6	32
none – natural	^{40}K	$1.3 \cdot 10^9$ yr	1460.8	1.3	6.6	7.4
^{238}U – natural	^{214}Bi	19.9 min	1764.5	1.6	4.4	15
^{232}Th – natural	^{208}Tl	3.05 min	2614.5	0.7	7.9	28

Tab. S2 Details about γ-spectrometry. For each of the analysed nuclides the relevant analytical information is reported. B.R. corresponds to branching ratio. For the emission at 241 keV from ^{224}Ra (marked by an asterisk), a correction was needed to remove an interfering contribution from ^{214}Pb.